Originally published on: *Journal of Power Sources 488 (2021) 229375*
DOI: 10.1016/j.jpowsour.2020.229375
https://doi.org/10.1016/j.jpowsour.2020.229375

Review on Mechanisms and Recovery Procedures for Reversible Performance Losses in Polymer Electrolyte Membrane Fuel Cells

Jens Mitzel[1,*], Qian Zhang[1,2], Pawel Gazdzicki[1], K. Andreas Friedrich[1,2]

[1]: German Aerospace Center (DLR), Institute of Engineering Thermodynamics, Pfaffenwaldring 38-40, 70569 Stuttgart, Germany
[2]: University of Stuttgart, Institute of Building Energetics, Thermal Engineering and Energy Storage (IGTE), Pfaffenwaldring 31, 70569 Stuttgart, Germany
*: Jens.Mitzel@dlr.de, telephone: +49 711 6862 8063, fax: +49 711 6862 747

Abstract

The recovery of performance losses in polymer electrolyte membrane fuel cells due to reversible degradation phenomena is an important topic to enable high system efficiency, reliable performance benchmarking and specific material improvement for a given application. Detailed knowledge of both, the sources for reversible performance loss and corresponding recovery mechanisms, are required to achieve cost and durability targets for fuel cell commercialization. This review paper provides a detailed overview of the mechanisms responsible for reversible performance losses. Moreover, it presents general requirements for the recovery of these losses and summarizes specific recovery procedures available in the literature. Eventually, it provides recommendations how to recover the performance loss caused by a certain reversible degradation mechanism. The study is aiming to present general recommendations for suitable recovery strategies and procedures for reliable testing in laboratories and for improved efficiency of operating systems.

Keywords

Recovery, Polymer Electrolyte Membrane Fuel Cell, Reversible Performance Losses, Reversible Degradation, Procedures, Mechanisms

Originally published on: *Journal of Power Sources 488 (2021) 229375*
DOI: 10.1016/j.jpowsour.2020.229375
https://doi.org/10.1016/j.jpowsour.2020.229375

Content

Originally published on: *Journal of Power Sources 488 (2021) 229375*
DOI: 10.1016/j.jpowsour.2020.229375
https://doi.org/10.1016/j.jpowsour.2020.229375

1 Introduction

Polymer electrolyte membrane fuel cells (PEMFCs) are promising energy converters for mobile and stationary applications to realize the transition to a carbon free energy supply of the transport and the energy sector [1]. Many barriers to widespread commercialization have been overcome during the last decades. Nowadays, more and more business cases for fuel cell applications become profitable, as can be seen for the energy supply of residential houses, the recent generation of electric vehicles, trains, busses, and heavy duty handling units powered by PEMFCs [2].

Nevertheless, two main challenges are remaining for the PEMFC technology: (i) durability under relevant conditions, such as dynamic conditions in passenger cars and (ii) targeted costs to be competitive with internal combustion engines (ICE) [3]. One of the main contributions to PEMFC stack cost in case of mass production is the catalyst layer [4]. Therefore, to lower the cost the amount of expensive catalyst materials has to be reduced by lowering the electrode loading with platinum group metals (PGM). The required loading to achieve the cost targets for automotive application is as low as 6 g_{PGM} per passenger car or 0.0625 g_{PGM} per kW system output power [5]. Since Pt is classified as a critical raw material (CRM) by the European Commission [6], another motivation to reduce the PGM loading to around 6 g_{PGM} per car is to keep the amount of Pt in circulation constant in the transport sector when replacing ICE cars using PGMs in the exhaust system by fuel cell electric vehicles (FCEVs). The recent years have shown that such low PGM loadings are linked to great challenges in terms of durability and lifetime and increase the importance of recovery procedures for reversible performance losses [7-9].

In general, various degradation phenomena have been identified to limit the PEMFC lifetime [10, 11]: (i) chemical and mechanical damages of the polymer electrolyte in the catalyst layers and in the membrane, (ii) deterioration of the catalyst activity by morphological changes due to platinum dissolution, aggregation and detachment, (iii) changes in the catalytically active surface due to platinum oxidation and adsorption of impurities, (iv) changes in the structural electrode properties by carbon corrosion to CO_2, and (v) changes in the water management due to formation of hydrophilic oxide species on the carbon support material. Thereby, the main focus over the last decade was on the understanding and mitigation of the effects associated to irreversible performance losses.

However, it is well known that idling and shut-down phases can have a positive impact on cell voltage and thus on the performance output of a PEMFC. Consequently, some of the effects resulting in performance decay during fuel cell operations can be considered as recoverable performance losses, often denominated reversible degradation effects [12] which is an imprecise term as they can be a consequence of material ageing which is often not reversible. Here we will use the term rate of reversible degradation for the rate of (irreversible) material changes leading to performance losses which can be recovered. Under harsh operation conditions, the rate of reversible performance loss is often even higher than irreversible degradation rates [9]. While irreversible performance losses can only be avoided by specific operation strategy and material improvement, the reversible performance losses can be recovered by specific procedures. Test procedures have been developed to evaluate the effect of reversible and irreversible degradation on fuel cell behavior during operation [3, 13-15]. These procedures are using defined test blocks of fuel cell operation under specific load cycles and recovery phases between the test blocks to recover the reversible performance loss (Figure 1). Reversible degradation is thereby characterized by non-linear voltage decay during the first hours after recovery and restart [13, 16]. It was demonstrated that this exponential contribution has a significant impact on fuel cell performance and usable power output under dynamic conditions, e.g. for automotive

Originally published on: *Journal of Power Sources 488 (2021) 229375*
DOI: 10.1016/j.jpowsour.2020.229375
https://doi.org/10.1016/j.jpowsour.2020.229375

applications. Hence, detailed understanding of reversible degradation effects and procedures for recovery of related performance losses are of particular interest and are still under discussion in the literature. The development of reliable and efficient recovery procedures can thereby enable: (i) high system efficiency if recovery phases can be included in the operation strategy [17], (ii) reliable performance evaluation for component benchmarking and differentiation between reversible and irreversible degradation rates [18], and (iii) understanding of reversible degradation effects which supports the development of new materials [19, 20].

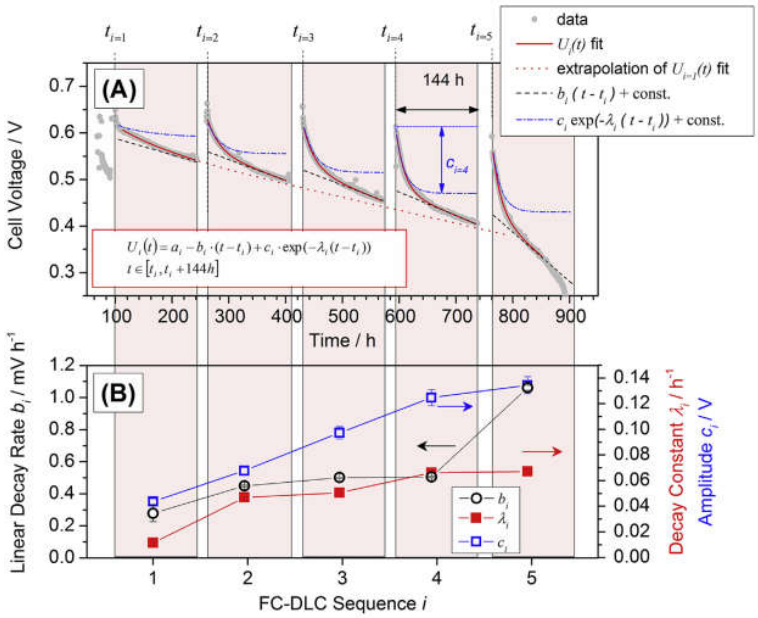

Figure 1: Degradation behavior using defined test blocks of 150 hours fuel cell dynamic load cycling (FC-DLC) interrupted by performance recovery. Results are shown for the cell voltage at 1.0 A cm^{-2}. (A) Cell voltage changes during degradation time and (B) results for linear decay rate b_i as well as decay constant λ_i and amplitude c_i for the exponential decay term indicated in (A). Reprinted from [13] with permission from Elsevier.

When designing recovery procedures not only for the laboratory but also for specific system operations, it is important to consider the constraints of a PEMFC system [21]. This results in the following requirements: (i) recovery has to be achieved under PEMFC system-relevant operating conditions (temperature, pressure, humidity), (ii) only reactants and conditions should be used, which are available in the system, (iii) fast recovery or recovery during shut-down is required to minimize not usable operation period and losses in efficiency.

The aim of this work is to provide a review of potential sources for reversible degradation in PEMFCs and to propose requirements for specific recovery procedures. Thereby, the focus is on state-of-the-art low temperature PEMFC systems fed with hydrogen and air. The PEMFC stacks consist of: (i) membrane electrode assemblies (MEAs) composed of perfluorosulfonic acid (PFSA) based membranes and ionomers, carbon-supported platinum catalysts, carbon-based gas diffusion layers as well as (ii) bipolar plates either graphite-composite or metallic. The presented mechanisms for reversible voltage decay are focused on these materials and the recovery strategies in this review can be efficiently applied to systems using components based on these materials. Not covered in this review are PEMFCs operating with reformate as hydrogen source, alloy catalyst, alternative catalyst support materials and

Originally published on: *Journal of Power Sources 488 (2021) 229375*
DOI: 10.1016/j.jpowsour.2020.229375
https://doi.org/10.1016/j.jpowsour.2020.229375

alternative ionomers. The degradation mechanisms and the recovery strategies might be different for such materials. It should be noted that all electrochemical electrode potentials mentioned in this paper are referred to the reversible hydrogen electrode (RHE).

2 Catalyst surface oxidation

2.1 Reversible degradation of platinum catalysts

The state-of-the-art catalyst platinum tends to oxidize in air at electrode potential above 0.7 V. Thus, PEMFC cathodes are subjected to conditions promoting oxidation especially under low load and high voltage operation [22]. This harmful operation is minimized in automotive fuel cell systems by applying the so-called voltage cut-off technology, focusing on controlling the cell potential and on minimizing the formation of Pt surface oxide layers [23]. The technology keeps the voltage of the fuel cell under a certain voltage threshold by assuring a small current during operation, e.g. by the use of resistors or by a small power consumption of the system components. Nevertheless, platinum oxidation is a significant source for reversible performance loss. It has been shown that oxide layers on platinum passivate the catalytic active surface and protect platinum from further oxidation at high potentials, but resulting in performance losses [24-26]. Platinum oxidation is of great importance for oxygen reduction reaction (ORR) kinetics because the Pt surface is partially oxidized in such conditions and oxygen cannot react effectively [27]. Consequently, the ORR rate is decreased. The involved reactions for the formation of platinum surface oxides are mainly considered being reversible as shown in Figure 2 (A). Only platinum dissolution to free ions is stated as irreversible. Several oxide species are associated to recoverable performance losses in the literature: (i) Pt-O [28], (ii) Pt-O_2 [29], (iii) Pt-OH [30], and (iv) Pt-OOH [31]. The nature of the surface oxide species and the kinetics of oxide formation and oxide reduction are important to understand the effect of performance losses and to apply appropriate recovery procedures for oxidized cathode catalysts [32-34].
There are two general possibilities for the formation of platinum oxides. The first is an electrochemical potential depending reaction using water as oxygen source [32, 35]:

$$\mathrm{Pt} + \mathrm{H_2O} \leftrightarrow \mathrm{Pt\text{-}OH} + \mathrm{H^+} + \mathrm{e^-} \quad \text{with } \mathrm{E^0} = 0.7\ \mathrm{V}, \tag{1}$$

$$\mathrm{Pt\text{-}OH} \leftrightarrow \mathrm{Pt\text{-}O} + \mathrm{H^+} + \mathrm{e^-} \quad \text{with } \mathrm{E^0} = 0.8\ \mathrm{V}. \tag{2}$$

The second option is a mixed chemical and electro-chemical reaction using O_2 as oxygen source [27]:

$$\mathrm{Pt} + \mathrm{O_2} \rightarrow \mathrm{Pt\text{-}O_2}, \tag{3}$$

$$\mathrm{Pt\text{-}O_2} + \mathrm{H^+} + \mathrm{e^-} \rightarrow \mathrm{Pt\text{-}HO_2}, \tag{4}$$

$$\mathrm{Pt\text{-}HO_2} + \mathrm{Pt} \rightarrow \mathrm{Pt\text{-}OH} + \mathrm{Pt\text{-}O}. \tag{5}$$

Three studies have shown that cathode potential and the water vapor pressure are key parameters to determine which oxidation pathway dominates [27, 35, 36]. Paik et al. [36] have demonstrated that below the potential threshold for water oxidation (equation (1)) O_2 is the main source for Pt oxidation and the extent of oxidation is directly proportional to oxygen concentration on the cathode. Above this threshold the oxygen concentration has no significant impact on extent of oxidation and water can be an additional oxygen source for platinum oxidation [36]. Thereby, the oxide formation using H_2O is

Originally published on: *Journal of Power Sources 488 (2021) 229375*
DOI: 10.1016/j.jpowsour.2020.229375
https://doi.org/10.1016/j.jpowsour.2020.229375

enhanced with increasing water vapor pressure because H_2O is directly involved in reaction (1) [27]. Thus, the share of oxides formed from water increases with increasing humidity, temperature, pressure and electrode potential as well as with decreasing oxygen concentration. As a consequence, surface oxide formation is facilitated at high humidity, high temperature, high electrode potential, and high oxygen content [37]. A crucial aspect of reversible performance losses due to platinum oxidation is the nature of the formed oxide [32], and the kinetic of the oxide reduction and performance recovery. While the hydroxide formation following equation (1) is fast and reversible, the formation of the oxide via equation (2) is slow and considered to be irreversible [38]. Both reactions result in a 2D surface monolayer of oxide species and reduce the ORR kinetic. According to Conway's theory [38] and experimentally proven by Teliska [32], a post-electrochemical slow and irreversible place exchange reaction between Pt surface atoms and surface oxygen species appears at potentials above 1.05 V. This reaction can reconstruct the platinum surface and form a subsurface oxide resulting in a 3D growth of the oxide layer. Due to the slow kinetic of oxide formation and place exchange, the Pt oxide film growth is following a direct logarithmic law as a function of time and electrode potential [33, 38]. Thus, the thickness of the oxide film and the surface coverage with oxide is depending on the time the cathode is exposed to oxidative conditions in the range of seconds to minutes [27, 36]. Potentials above 0.8 V are present during PEMFC operation in idling phases and potentials above 1.05 V are locally possible, e.g. due to non-uniform behavior during start/stop [27]. The formed 3D oxide film has shown to be electrochemically more stable and recovery procedures are required for oxide reduction [24, 38].

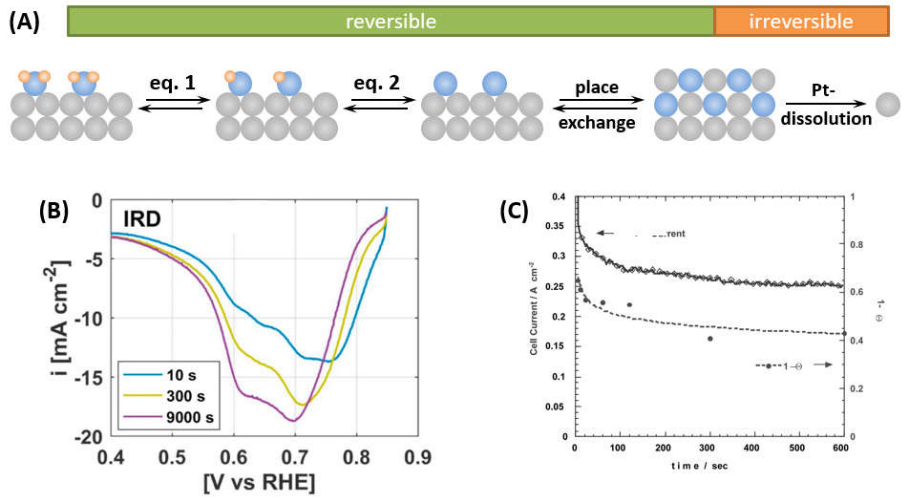

Figure 2: (A) Reversible and irreversible oxidation reactions of platinum. (B) Linear sweep voltammetry after oxidation at 0.85 V in N_2 for different hold times, reprinted from [37] with permission from Elsevier. (C) Cell current density and degree of OH-free Pt surface at 0.8 V, reprinted from [39] with permission from Elsevier.

2.2 Requirements for performance loss recovery caused by platinum oxidation

In general, the formed oxide species on Pt can be reduced back to metallic platinum depending on the electrode potential and on the surrounding atmosphere [10, 40, 41]. It is reported that platinum oxide formation strongly contributes to the recoverable performance losses [37]. The required recovery conditions depend on the nature of the formed platinum oxide. After mild oxidation (only 2D oxide layer), surface diffusion and reduction recover the platinum surface fast with little reconstruction at

Originally published on: *Journal of Power Sources 488 (2021) 229375*
DOI: 10.1016/j.jpowsour.2020.229375
https://doi.org/10.1016/j.jpowsour.2020.229375

potentials below 0.7-0.8 V. But after more extensive oxidation including place exchange reaction, reduction will occur after limited surface diffusion, leading to a more reconstructed final surface. This results in a slow and challenging recovery process [33]. The formed 3D Pt-oxide has shown to be electrochemically more stable and low electrode potentials are required for reduction and Pt surface recovery [38]. Exposure of such a oxidized Pt surface to open circuit conditions in a nitrogen atmosphere (using hydrogen on the anode) for 3 h does not remove oxidized products indicating that the recovery process is very slow [27]. The kinetic model developed by Darling and Meyers confirms the slow reaction kinetic of both, platinum surface oxidation and oxide reduction [26]. In general, reductive environment is required for removal of the platinum oxide which can be provided by low cathode potentials and can be promoted by the presence of hydrogen on the cathode. It was found that 3D oxide layers formed by place exchange reaction are only reducible in the potential region corresponding to underpotential deposition of hydrogen below 0.4 V [34, 38]. Thereby, the formed oxide layer can be removed following two different reactions, depending on the surface coverage with oxygen. When the majority of the surface is covered (θ>0.6) the active sides for a electrochemical reaction are blocked and a slow chemical reaction with hydrogen is required for oxygen removal [34]:

$$2\ \text{Pt-O} + \text{H}_2 \rightarrow 2\ \text{Pt-OH} \rightarrow \text{Pt-O} + \text{Pt} + \text{H}_2\text{O} \tag{6}$$

As soon as enough free platinum sides are available (θ < 0.6) a fast electrochemical reaction with the hydrogen oxidation reaction (HOR) as source for electrons accelerated the recovery process [34]:

$$2\ \text{Pt} + \text{H}_2 \rightarrow 2\ \text{Pt-H} \rightarrow 2\ \text{Pt} + 2\ \text{H}^+ + 2\ \text{e}^- \tag{7}$$

$$\text{Pt-O} + 2\ \text{H}^+ + 2\ \text{e}^- \rightarrow 2\ \text{Pt} + \text{H}_2\text{O} \tag{8}$$

The combination of both reactions can enable complete removal of the oxygen species and thus full recovery of the performance loss. Thereby, the required recovery time is depending on the oxidation conditions during the performance loss and was determined to be in range of several seconds [34].

2.3 Recovery procedures for platinum oxidation

Different publications have demonstrated that full recovery of the performance loss can be achieved by cyclic voltammetry (CV) feeding nitrogen to the cathode and hydrogen to the anode and applying potential cycling down to 0-100 mV with moderate scanning rates of 10-50 mV/s [26, 27, 34-38, 42]. Thereby the charge for platinum oxide reduction increased with the extent of surface oxidation as a function of operating conditions and hold time at high potentials. Paik et al. [36] have demonstrated that the CV is shifted to reductive, negative current over the entire potential range after the formation of highly stable 3D oxide layers. This shows the slow kinetic for the reduction of such oxide layers, which is not completed in the reductive scan and several cycles are required for full oxide removal. Zago et al. [37] have referred an additional oxide reduction peak at 0.61 V to the reduction of this highly stable oxide species (Figure 2 (B)). They have shown that this stable oxide species has a more significant impact on decrease of specific ORR activity compared to weak bond surface oxides.
Because recovery requires low potentials, Zhang et al. have applied low potential steps of 0.2 V for 5 minutes in nitrogen atmosphere [43]. Up to 10 steps were required to restore the initial electrochemical active surface area (ECSA) and achieve almost full recovery of the kinetic losses caused by platinum oxidation. Thereby, a major part of the losses was recovered rapidly in the first step while

Originally published on: *Journal of Power Sources 488 (2021) 229375*
DOI: 10.1016/j.jpowsour.2020.229375
https://doi.org/10.1016/j.jpowsour.2020.229375

remaining losses are recovered slowly in the subsequent steps. The latter might be an indication for the formation of highly stable platinum oxides and the slow kinetic of their reduction as stated above. Cyclic voltammetry and low voltage steps in nitrogen atmosphere can be applied in laboratories, but not in operating systems. An alternative recovery procedure for oxidized cathode catalysts is the short-term operation at high current density and low cell voltage. Owejan et al. have reported full recovery of reversible performance losses by 2 hours of fuel cell operation at 0.3 V and have demonstrated that reliable recovery procedures for oxidized platinum catalyst are highly important for low loaded electrodes [44]. Zago et al. [37] have shown that shorter low voltage operation of 0.3 V at 1.2 A cm^{-2} for 1 minute can recover 85% of the performance losses after mild oxidation conditions at 0.7 V and 65% after severe oxidation conditions at 0.85 V by oxide removal and thus decreased charge transfer resistance for ORR in impedance spectra. Uribe et al. have applied even shorter low voltage periods of 0.2 V at 1.4 A cm^{-2} for up to 6 seconds with a duty cycle of 1% during long-term PEMFC operation at 0.8 V [39]. It was demonstrated that both, the performance loss at this potential and the coverage of the platinum surface with oxides, can be mitigated by the applied pulses (Figure 2 (C)). Full recovery is reported in this work, but in contrast to the experiments of Zago et al. [37] the oxides are reduced constantly and shortly after surface oxidation. Due to the slow kinetic of the formation of the highly stable platinum oxide layers, it can be assumed that only weakly adsorbed oxygen species are formed under these conditions.

The formed platinum oxides cannot be reduced only electrochemically, but also chemically by hydrogen entering the cathode after cell shut-down following equation (6). Hydrogen can enter the cathode by permeation through the membrane from the anode side. Dhanushkodi et al. have applied this technique for 20 minutes to 4 hours to a single cell fed by hydrogen on the anode and nitrogen on the cathode to recover all reversible performance losses [45, 46]. Zago et al. [37] have shown that this method can also be applied without nitrogen atmosphere when the air feed is stopped and the hydrogen feed is maintained. It was demonstrated that hydrogen permeation results in a cathode potential below 0.2 V and that 2 minutes of recovery under such conditions is more effective than electrochemical recovery by current pulses or by voltage cycling. Nevertheless, full recovery could not be achieved and the resulting losses are referred to catalyst interaction with ionomer (see section 4). Further improvement of the recovery procedure using hydrogen was demonstrated by Choo et al. [47]. Purging the cathode with hydrogen was compared to an electrochemical hydrogen pump using a power supply and the latter was found to accelerate the recovery effect by a factor of 10. This demonstrates that the generation of highly active hydrogen directly on the platinum surface in combination with the low cathode potential of lower than 100 mV during hydrogen pumping can improve oxide reduction and increase the slow kinetic. This method was also patented by Choo et al. and the Hyundai Motor Company in 2018 for the direct application in a fuel cell electric vehicle (FCEV) without modification of the system components [48]. Thereby, it was demonstrated that stack cooling to 15-30 °C is beneficial for the performance recovery.

It can be concluded that the formation of 3D oxide films and the slow kinetic of their reduction result in the need of recovery procedures for performance losses caused by platinum oxidation. The combination of low electrochemical potential (<0.3 V) and a reductive atmosphere at the cathode using hydrogen is the most suitable procedure in laboratories and systems. The hydrogen can be provided to the cathode by permeation from the anode when the air supply is interrupted. To accelerate the recovery, the cell can be operated in hydrogen pump mode, but this requires the use of a power supply.

Originally published on: *Journal of Power Sources 488 (2021) 229375*
DOI: 10.1016/j.jpowsour.2020.229375
https://doi.org/10.1016/j.jpowsour.2020.229375

3 Contamination of catalyst surface

Nowadays, steam methane reforming (SMR) from natural gas and biomass is still the dominant method for hydrogen production [49, 50]. SMR results in unavoidable impurities in the hydrogen fuel, even at low levels. Additional sources for contaminants are combustion products in the air from automotive vehicle exhaust and industrial manufacturing processes. Cheng et al. [51] have summarized contaminants with impact on PEMFC performance. Thereby, the impact can be categorized by: (i) kinetic losses due to the catalyst poisoning, (ii) ohmic losses due to resistance increase of cell components, and (iii) mass transport losses due to changes in structure and hydrophobicity of components [52, 53]. Table 1 summarizes contaminants causing reversible and recoverable performance losses in PEMFCs. The listed contaminants are limited to the everyday use of hydrogen/air PEMFCs and special contaminants, such as battlefield contaminants (e.g. sarin, hydrogen cyanide) [54] are neglected. Furthermore, the impact of contaminants from system components and manufacturing processes (e.g., urethan, silicon, hexanediol) [55, 56] as well as air contaminants in industrial environment (e.g. benzene, naphthalene, propene, methyl methacrylate) [57, 58] are not covered in this review. Detailed information on these contaminants can be obtained from the included references.

Table 1: Contaminants causing reversible performance losses in PEMFCs.

Impurity Source	Classification	Contaminant	Mechanism	Impact
Air	Nitrogen contaminants	NO_x: NO, NO_2	Catalyst poisoning	Kinetic
		NH_3	Membrane poisoning	Ohmic, kinetic
	Sulfur contaminants	SO_x: SO_2, SO_3 H_2S COS	Catalyst poisoning	Kinetic
Hydrogen	Carbon contaminants	CO_x: CO, CO_2	Catalyst poisoning	Kinetic
	Sulfur contaminants	H_2S	Catalyst poisoning	Kinetic
Bipolar plate	Metal ions	Fe^{2+}, Fe^{3+}, Ni^{2+}, Cu^{2+}, Cr^{3+}	Membrane poisoning	Ohmic
Membrane	Degradation products	SO_4^{2-}	Catalyst poisoning	Kinetic
	Metal ions	Na^+, Ca^{2+}	Membrane poisoning	Ohmic

In the following, catalyst poisoning by contaminants with impact on the catalyst kinetic is described. Sulfur contaminants H_2S, SO_2 and carbonyl sulfide (COS) and decomposition products from membrane degradation such as sulfonate and sulfate ions can adsorb on the catalyst surface in PEMFC electrodes and can result in sluggish ORR kinetics at the cathode catalyst [41, 59]. Further contaminants with recoverable impact on the fuel cell kinetic and performance are NO_x as well as CO and CO_2. As Figure 3 (A) demonstrates, voltage decay caused by sulfur compounds was found to be much more severe than that by nitrogen compounds [60]. Thereby, the oxidation state of sulfur compounds, SO_2 or H_2S, seems not to affect the performance decay rate. Performance losses due to sulfur compounds can only

Originally published on: *Journal of Power Sources 488 (2021) 229375*
DOI: 10.1016/j.jpowsour.2020.229375
https://doi.org/10.1016/j.jpowsour.2020.229375

be recovered partially by fuel cell operation with neat air, while losses caused by nitrogen compounds can be almost completely recovered [61].

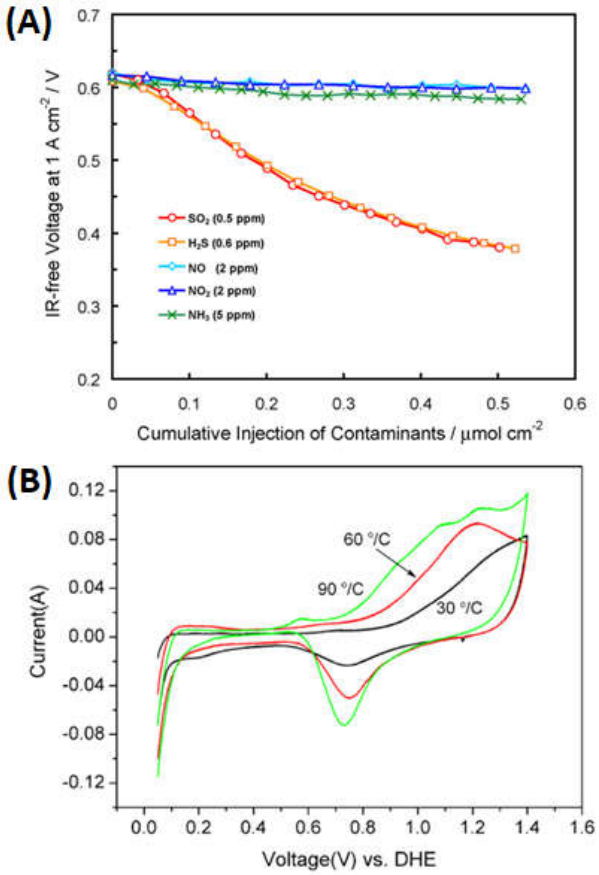

Figure 3: (A) Effect of various air contaminants on the cell voltage at 1 A cm^{-2}, reprinted from [60] with permission from Elsevier. (B) Cyclic voltammetry of a PEMFC anode using a Pt catalyst after exposure to 500 ppm H_2S at different temperatures, reprinted from [62] with permission from Elsevier.

The following sections will highlight the reason for performance losses and the possibility to recover these losses for each contaminant.

3.1 Adsorbed sulfur species from external impurities

3.1.1 Reversible degradation caused by sulfur species

The sulfur-containing airborne contaminants SO_2, H_2S and COS can provoke reversible voltage losses in PEMFCs [63]. Additionally, H_2S can be also available as a contaminant in the hydrogen feed. The poisoning effect of H_2S on Pt catalysts was reported to be a result of Pt surface coverage by sulfur. H_2S is strongly adsorbed to the Pt surface and dissociated under formation of platinum sulfide which blocks the active sides of the catalyst. In the literature the dissociative mechanisms are referred to either chemical decomposition [64] described by

Originally published on: *Journal of Power Sources 488 (2021) 229375*
DOI: 10.1016/j.jpowsour.2020.229375
https://doi.org/10.1016/j.jpowsour.2020.229375

$$H_2S + Pt \rightarrow Pt\text{-}SH_2 \quad (9)$$

$$Pt\text{-}SH_2 \rightarrow Pt\text{-}S + H_2 \quad (10)$$

or electrochemical oxidation [65] according to

$$H_2S + Pt \rightarrow Pt\text{-}S + 2\,H^+ + 2\,e^- \quad \text{with } E^0 = 0.30\ V \quad (11)$$

This poisoning effect could be detected at anode and cathode in fuel cell operation. The impact on the cathode was explained by crossover of the H_2S in the hydrogen fuel from anode to cathode across the membrane due to H_2S water solubility [66] or H_2S as an airborne contaminant. The effect on the anode was studied by Garzon et al. by exposing 0.5 ppm H_2S for 2.5 h to the anode during hydrogen pumping operation to determine anodic polarization losses without impact of the ORR [67]. It was shown that the anodic overpotential increased by about 75 mV at 1 A cm^{-2} and these losses were confirmed in fuel cell operation. Additionally, stripping voltammetry confirmed Pt-S as poisoning species.
Another source for sulfur poisoning of the catalyst surface is SO_2 available as a contaminant in the air feed. The poisoning effect of SO_2 is the same as for H_2S. SO_2 is dissociated and the formation of platinum sulfide is the reason for the blockage of the active sides of the catalyst. In contrast to H_2S, the formation of the platinum sulfide from SO_2 is the result of an electrochemical reduction on the catalyst surface [68]:

$$SO_2 + Pt + 2\,H^+ + 2\,e^- \rightarrow Pt\text{-}SO + H_2O \quad (12)$$

$$Pt\text{-}SO + 2\,H^+ + 2\,e^- \rightarrow Pt\text{-}S + H_2O \quad (13)$$

In aqueous solution this reaction requires a potential range of 0.21 to 0.45 V [68] and in PEMFCs environment a range of 0.05 to 0.1 V is reported [47].
The poisoning effect of COS on Pt catalysts is referred to a dissociative chemisorption on the catalyst surface. This mechanism was examined in a spectroscopic study using a Pt/Al_2O_3 catalyst [69] and is described by

$$Pt + COS \rightarrow Pt\text{-}COS \quad (14)$$

$$Pt\text{-}COS + Pt \rightarrow Pt\text{-}CO + Pt\text{-}S \quad (15)$$

3.1.2 Requirements for performance loss recovery caused by sulfur species

Due to the same poisoning species Pt-S, all three contaminants H_2S, SO_2, and COS show comparable poisoning and recovery behavior [63]. The poisoning rate is strongly depending on the contaminant concentration, and after poisoning the performance can only be partially recovered by fuel cell operation in neat hydrogen and air without contaminants [70]. Consequently, the recovery of performance losses due to sulfide poisoned catalysts requires special recovery procedures. The removal of the platinum sulfide is only possible by oxidative desorption. It was reported that two distinct oxidation peaks can be identified in CV measurements during such procedures [71]. In aqueous solution, two forms of chemisorbed sulfur were identified distinguishable by the number of platinum sites occupied per sulfur atom [72]. They are attributed to the oxidation of linear-bonded, weakly chemisorbed sulfur at 0.97 V and to the oxidation of bridge-bonded, strongly chemisorbed sulfur at 1.1 V. During recovery procedures in PEMFC the potentials of the reactions are reported between 0.9

Originally published on: *Journal of Power Sources 488 (2021) 229375*
DOI: 10.1016/j.jpowsour.2020.229375
https://doi.org/10.1016/j.jpowsour.2020.229375

V and 1.3 V depending on the operating conditions [62, 70, 71, 73, 74]. Both oxidation reactions can result in the formation of SO_3 or SO_4^{2-} [75] according to:

$$\text{Pt-S}_{\text{ads}} + 4\,\text{H}_2\text{O} \rightarrow \text{Pt} + \text{SO}_4^{2-} + 8\,\text{H}^+ + 8\,\text{e}^- \quad (16)$$

$$\text{Pt-S}_{\text{ads}} + 3\,\text{H}_2\text{O} \rightarrow \text{Pt} + \text{SO}_3 + 6\,\text{H}^+ + 6\,\text{e}^- \quad (17)$$

As a consequence, sulfur poisoning requires high electrode potentials for oxidative removal of the sulfide species. However, cathode potentials higher than 1 V are difficult to achieve upon nominal PEMFC operation. Furthermore, the resulting sulfate anions can also adsorb on the catalyst surface and decrease the performance of the fuel cells [76]. The removal of the sulfate ions requires other recovery procedures as discussed in section 3.2.

3.1.3 Recovery procedures for sulfide contamination

Several procedures were established to recover performance losses caused by sulfide poisoning. The most common procedure is the use of CV. Typically, the potential is cycled between 0.0 and 1.4 V using scan rates in the range of 5 to 20 mV s^{-1}. Thereby, the poisoned electrode is exposed to nitrogen while the other electrode is exposed to hydrogen to enable reliable control of the electrode potential. It was demonstrated that this method can fully recover the appearing voltage losses caused by H_2S contamination in the anode and the cathode [62, 70, 71, 73] and by SO_2 contamination in the cathode [70]. However, depending on the operating conditions, several cycles are required for full recovery. Shi et al. [62] have demonstrated that the increase of the cell temperature was beneficial for sulfide oxidation and removal. It was shown that the onset potential can be lowered, and the oxidation charge can be increased if the cell temperature is increased from 30 to 90°C (Figure 3 (B)).

To accelerate the performance recovery after sulfur poisoning, Shi et al. applied potential pulses on a H_2S poisoned electrode under similar conditions as used for the CV recovery, namely under nitrogen and hydrogen atmosphere [74]. The pulses were applied for 20 to 120 s at 1.5 V and at 0.2 V each. Ten pulses were required for full recovery and the method was demonstrated in a single cell and in a stack. For stack recovery, this pulse method as well as the CV method has to be applied to each single cell individually.

This limitation of both methods to single cells and the required access to nitrogen as well as to an external power supply prevent the application in operating systems while providing reliable recovery methods for sulfur poisoning in laboratory tests. Urdampilleta et al. [73] have investigated alternative methods to increase the potential of sulfur poisoned electrodes without these limitations. Recovery of cathode poisoning was achieved using open circuit voltage (OCV) phases under fuel cell conditions applying hydrogen and air to anode and cathode, respectively. The performance recovery showed time dependency and recovery rates of 72% after 0.5 h, 80% after 1 h, and 92% after 3 h were achieved. Consequently, almost complete recovery of sulfur poisoned cathodes can be achieved by long OCV periods. However, OCV conditions are also known to accelerate membrane degradation [52] and are mitigated in system operation as much as possible. Urdampilleta et al. [73] also investigated an air bleed OCV recovery procedure to remove sulfides from the anode by adding 8% of air to the hydrogen feed during OCV hold. No benefits in performance recovery were found.

A detailed study to identify efficient recovery procedures of sulfur contaminants was published by Gould et al. [21]. This work highlighted that not only the oxidation of Pt-S, but also desorption and removal of the resulting sulfate ions is of high importance for performance recovery. The high potential for oxidative Pt-S removal requires balancing of Pt-S oxidation and catalyst degradation due to Pt and

Originally published on: *Journal of Power Sources 488 (2021) 229375*
DOI: 10.1016/j.jpowsour.2020.229375
https://doi.org/10.1016/j.jpowsour.2020.229375

C oxidation. In accordance with [59], the optimum oxidation potential was determined to 1.1 V at 60 °C. Whereby, this value depends on the temperature and the used catalyst material. As presented in section 3.2, the removal of the sulfate ions as oxidation product of Pt-S requires low potential of about 0.1 V. The investigated recovery methods are summarized in Table 2 and following conclusion can be drawn from this study [21]:

- Appling high potentials (over 1 V) for Pt-S oxidation can only partially recover performance losses.
- Potential cycling between high potential of about 1.1 V for Pt-S oxidation and low potential of about 0.1 V for sulfate removal is essential for performance recovery. This also enables PtO reduction and regeneration of a sufficient number of free Pt metal sites necessary for sulfur oxidation.
- Recovery efficiency is independent from the applied scan rate. For high scan rates the recovery procedure can be significantly accelerated.
- An in-situ N_2 atmosphere by closed cathode compartment and electrochemical consumption of O_2 at 0.6 V can be applied to enable fast recovery and reduce occurring currents during potential cycling recovery.

Consequently, the potential cycling between 0.09 and 1.1 V in an in-situ N_2 atmosphere was identified to be the best recovery method. The method enables efficient recovery in the entire current density range within 3 minutes.

Table 2: Effectiveness of different recovery methods [21]

Recovery method	**Recovery time (min)**	**$P_{recovered}/P_0$ at 0.60 V**	**$P_{recovered}/P_0$ at 0.85 V**
Potential cycling with in-situ N_2 between 0.09 and 1.1 V	2.4	0.99	0.92
Potential hold with in-situ N_2 at 1.1 V	2.7	0.92	0.73
Potential cycling in air between 0.09 and 1.1 V	30	0.99	0.98
Potential hold in air at 1.1 V	2.7	0.92	0.73
Load cycling in air	4800	0.91	0.72
No recovery	N/A	0.79	0.71

In summary, high electrode potentials have to be applied to recover performance losses due to sulfur poisoning caused by H_2S, SO_2, and COS contaminants to oxidize Pt-S on the catalyst surface. Subsequently, the formed sulfate anions have to be desorbed and removed from the catalyst under low potential. Potential cycling using nitrogen proposes a reliable procedure for laboratory tests and can be converted to systems by the use of an in-situ nitrogen atmosphere by electrochemically consuming the oxygen on the cathode. Nevertheless, efficient recovery in PEMFC systems requires the use on an external power source to apply the required electrode potential range from 0.1 to 1.1 V.

3.2 Sulfate and sulfonate anions from the ionomer

3.2.1 Reversible degradation by sulfate and sulfonate anions

Sulfate anions can be not only a result of sulfur contaminants as stated previously, but also a product of ionomer degradation. Low load operation of PEMFCs, such as idling and OCV conditions, is known to accelerate chemical degradation of membranes especially under low humidification [52]. This

Originally published on: *Journal of Power Sources 488 (2021) 229375*
DOI: 10.1016/j.jpowsour.2020.229375
https://doi.org/10.1016/j.jpowsour.2020.229375

degradation is caused by attack of peroxi-radicals produced at the anode catalyst surface due to oxygen crossover from the cathode side [77]. The state-of-the-art materials for membranes are based on PFSA. The decomposition of these membranes generates various compounds including fluoride, sulfate, and low-molecular-weight organic sulfonic acids mainly by chemical attack at the side chains [78-80]. Organic sulfonic acids can be released through chain scission and unzipping of the side chain from the polymer backbone [78, 79]. The release of sulfate can be explained by mechanisms in which degradation by the oxygen radicals initiated directly from the $-SO_3H$ end group, thus releasing sulfate ions [81, 82]. Sulfate or sulfuric acid is supposed to be the most poisoning decomposition product from the membranes. The anion adsorbs on the cathode catalyst surface, leading to a large mass activity reduction and performance drop [78, 79]. This contamination was proposed as the mechanism that accounts for the reversible voltage loss observed during OCV holds [83], thus under conditions promoting the chemical membrane degradation. CV studies in sulfuric acid [78] and in PEMFC after OCV test [84] show significant impact of adsorbed sulfate on surface behavior of platinum catalysts. The hydrogen adsorption/desorption region as well as the onset potential for the formation of platinum oxide species are affected, what is expected to be the reason for the lowered mass activity of the catalyst.

3.2.2 Requirements for performance loss recovery caused by sulfate and sulfonate

It was demonstrated that this sulfonate adsorption is reversible and that the resulting performance loss is fully recoverable [85]. The adsorption of sulfate anions is a result of coulombic interactions with the positively charged electrode. The recovery of the performance loss due to desorption of the sulfate ions can be achieved below the potential of zero charge which is reported to be 0.17 V [86]. For effective sulfate desorption in PEMFC applications, potentials below 0.3 V [87] are required, preferably potentials of about 0.1 V are applied [47]. While these electrode potentials are easy to achieve on the hydrogen fed anode, the cathode potentials are significantly higher during fuel cell operation. Consequently, SO_4^{2-} mainly affects the cathode and ORR activity is significantly decreased as shown in measurements in $HClO_4$ and H_2SO_4 solution [88]. Different procedures were evaluated for the removal of adsorbed sulfate ions on the cathode surface.

3.2.3 Recovery procedures for sulfate and sulfonate contamination

Sugawara et al. [83] applied low cathode potential under condensing conditions to remove the adsorbed sulfate after an OCV degradation test, promoting membrane degradation and sulfate adsorption. A single cell was fed with hydrogen and nitrogen with a dew point of 80 °C to the anode and the cathode, respectively. The cell was operated at 50°C. The cell was held at OCV conditions resulting in a voltage of about 0.1 V for 2 hours to desorb the sulfate anions and these anions were flushed out from the MEA due to the condensation operation. It was demonstrated that the performance loss was caused by lower ORR kinetic activity and thus by a reduction of active sides availability for ORR. Analysis of the exhaust water has shown that the membrane degradation products behave differently in the fuel cell. Fluoride emission was visible only during OCV degradation, but not during recovery. Consequently, fluoride anions do not absorb on the catalyst surface. On the contrary, sulfate release was detected primarily during the recovery phase which demonstrates that the sulfate anions are adsorbed during the OCV degradation test and are released during the recovery phase. Nevertheless, the applied recovery procedure only partially (about 30%) recovered the kinetic performance loss after OCV degradation test.

Originally published on: *Journal of Power Sources 488 (2021) 229375*
DOI: 10.1016/j.jpowsour.2020.229375
https://doi.org/10.1016/j.jpowsour.2020.229375

For full recovery, the authors suggested combining this method with high load fuel cell operation under fully humidified conditions to remove all sulfate ions from the MEA. This technique was applied by Nagahara et al. [60] in a study regarding H_2S and SO_2 contamination and recovery. After oxidation of these contaminants to sulfate ions at high potential the performance could only be partially recovered. To almost completely restore the cell performance a combination of low cathode potential and water condensation was applied by fuel cell operation at 80 °C at 1 A cm^{-2} using fully humidified hydrogen and oxygen at ambient pressure. Due to the production of water during fuel cell operation the remaining sulfate ions are dragged away from the catalyst surface and removed from the catalyst layer. These findings were confirmed by Inaba et al. [89], demonstrating sulfate ion accumulation under low humidification operation and sulfate ion wash-out due to condensed water under fuel cell operation with fully humidified reactants. Adsorption of sulfate anions onto the platinum catalyst during degradation at OCV and sulfate release during recovery phase was also demonstrated by General Motors [84, 85]. The applied recovery procedure is proprietary, requires about 2 hours and enables full recovery of the occurred voltage losses. No organic compounds were detected during recovery by total organic carbon analysis. Thus, no sulfonic acids were present and the SO_4^{2-} adsorption was solely identified to cause the performance loss of up to 120 mV at 1.5 A cm^{-2}. Thereby, about 30% of the released sulfate is absorbed and cumulatively covers the platinum surface.
Kabasawa et al. [90] have studied the effects of decomposition products from PFSA membranes. Only sulfonate ions could be detected as decomposition products. Under low humidity fuel cell conditions, these degradation products adsorb on the catalyst and accumulate in the cathode with severe impact on the performance. Full recovery by potential cycling in nitrogen atmosphere and subsequent fuel cell operation using fully humidified reactants was demonstrated. Thereby, the water produced at the cathode assisted the complete removal of adsorbates from the platinum catalyst surface. This study was confirmed by injecting membrane decomposition products in aqueous solutions to an operating PEMFC and by full recovery of the resulting performance losses by potential cycling and fuel cell operation at 1.0 A cm^{-2} using fully humidified H_2/O_2 [78].

Prass et al. [91] have demonstrated that sulfur poisoning by H_2S can also be recovered by cell shut-down und start-up after oxidation of these contaminants to sulfate ions. Condensing water during shut-down can dissolve the sulfate ions and remove the contamination during cell start-up. This effect is most pronounced at ultralow-loaded anodes due to low thickness of these electrodes and might be of high interest for next generation MEAs.

In summary, the recovery of performance losses caused by sulfate and sulfonate anions can be assured by desorption of the ions due to applying low potentials of about 0.1 V and a subsequent fuel cell operation using fully humidified reactants to remove the ions from the catalyst layer. Alternatively, sulfate anions can be removed from the cell by shut-down and start-up, at least for ultra-low loaded anodes.

3.3 Adsorbed nitrogen species from air impurities

3.3.1 Reversible degradation by nitrogen species

Nitrogen oxides (NO_x) are mainly released into the atmosphere as a combustion product of fossil fuels. They are typically emitted in the form of nitric oxide (NO) which can then be oxidized to nitrogen dioxide (NO_2). Elevated NO levels in air of 400 ppb are usually observed [54]. But NO_x concentration close to the exhaust of ICE vehicles can easily exceed 50 ppm, even up to 300 ppm [92]. Furthermore,

Originally published on: *Journal of Power Sources 488 (2021) 229375*
DOI: 10.1016/j.jpowsour.2020.229375
https://doi.org/10.1016/j.jpowsour.2020.229375

fuel cells applied to conditions with limited air ventilation, such as mining operation, can result in increased NO_x contaminant concentration [93]. Consequently, NO_x contamination can impact the fuel cell performance in different applications. Typically the NO_x composition is dominated by 85-95% NO and 5-15% NO_2 [92, 93], which are therefore investigated as potential contaminants with impact on the fuel cell performance.

Several studies regarding the impact of NO_x on the performance of PEMFCs have been reported. Moore et al. [54] and Nagahara et al. [60] demonstrated that exposure to NO_x concentrations below 2 ppm for short time (15 to 60 minutes) has a negligible effect. In contrast, Mohtadi et al. [70], Yang et al. [94] and Jing et al. [61] have shown that the intrusion of higher NO_x concentrations or longer exposure time results in fast performance loss up to 55% of the initial performance (Figure 4 (A)). The study of Chen et al. [95] analyzed the mechanism and recovery of NO_x poisoning in a three electrode setup using liquid electrolyte. It was shown that NO_x poisoning is caused by chemical adsorption rather than an electrochemical process and that this adsorption is more significant on metallic platinum than on platinum oxides. Consequently, performance losses by NO_x poisoning are more severe if the cathode is operated at potentials below 0.65 V. Kinetic measurements were used to prove that ECSA reduction is the reason for the decreased performance while the ORR mechanism remains almost the same.

Originally published on: *Journal of Power Sources 488 (2021) 229375*
DOI: 10.1016/j.jpowsour.2020.229375
https://doi.org/10.1016/j.jpowsour.2020.229375

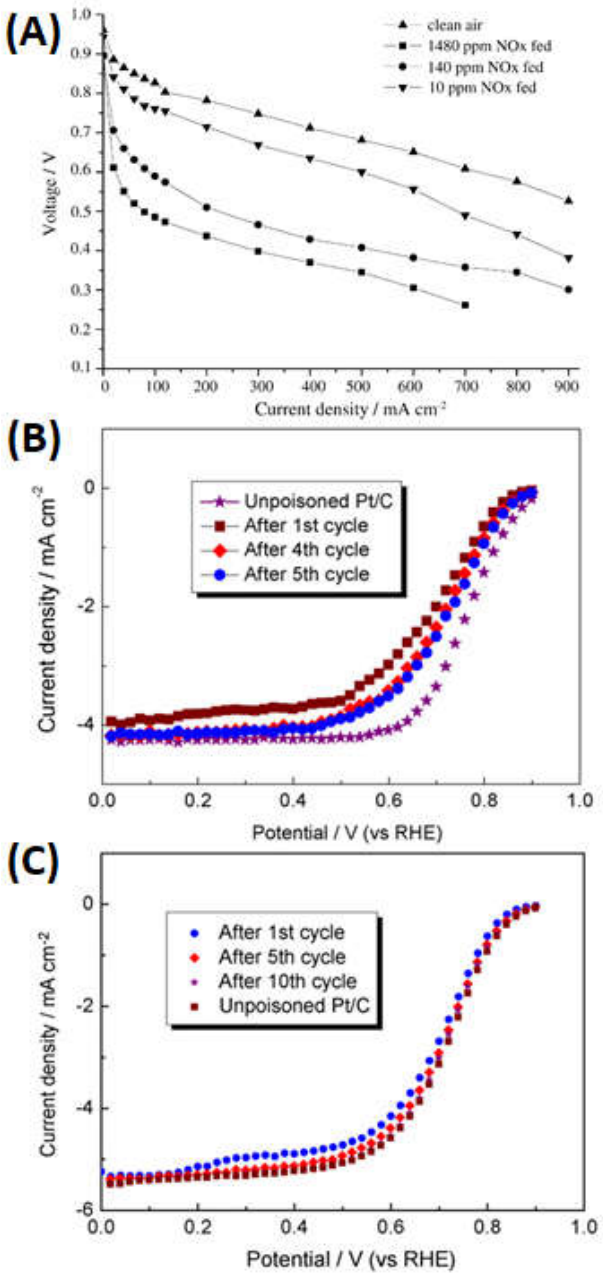

Figure 4: (A) Impact of different NO_x concentrations on the performance of a PEMFC single cell, reprinted from [94] with permission from Elsevier. Linear sweep voltammetry for a poisoned Pt/C catalyst (B) after reductive recovery and (C) after oxidative recovery, reprinted from [95] with permission from Elsevier.

3.3.2 Requirements for performance loss recovery caused by nitrogen species

In general, the adsorbed NO_x impurities can completely desorb from the cathode catalyst under fuel cell operation but this recovery process requires NO_x-free air and takes several hours [67, 70, 93, 94]. There are two electrochemical options to accelerate this recovery process. Potentials below 0.3 V result in NO_x reduction to water soluble ammonium ions (NH_4^+) [96, 97] according to

$$NO_x + (4 + 2x)\, H^+ + (3 + 2x)\, e^- \rightarrow NH_4^+ + x\, H_2O \qquad (18)$$

Originally published on: *Journal of Power Sources 488 (2021) 229375*
DOI: 10.1016/j.jpowsour.2020.229375
https://doi.org/10.1016/j.jpowsour.2020.229375

The disadvantages of the reductive recovery procedure are the slow kinetics of the NO_x reduction [98] and the fact that the reduction product NH_4^+ affects the ionomer which can result in further performance losses [99, 100] (see section 4.2).

In contrary, potentials above 0.9 V result in oxidation of NO_x to water soluble nitrate ions (NO_3^-) [61] according to

$$NO_x + (3 - x)\, H_2O \rightarrow NO_3^- + (6 - 2x)\, H^+ + (5 - 2x)\, e^- \quad (19)$$

Furthermore, mass spectroscopic studies have shown that NO can react with oxygen on Pt surface to NO_2 which can also be oxidized to nitrate [94]:

$$2\, NO + O_2 \rightarrow 2\, NO_2 \quad (20)$$

Finally, the nitrate anions can be dissolved into water and removed from the fuel cell without impact on the ionomer as discussed for ammonium ions.

Chen at al. have investigated reductive and oxidative removal of adsorbed NO_x in a 3 electrode setup using a liquid electrolyte [95]. It was demonstrated that the reductive current for NO_x reduction to ammonium overlaps in the region of 0.0 to 0.3 V with the hydrogen adsorption peaks. The ECSA could only be partially restored by potential cycling in the reductive potential region. The resulting ORR kinetic measurements have shown that the activity of the catalyst cannot be fully recovered by this method (Figure 4 (B)). On the other hand, oxidation of NO_x to nitrate was verified by the presence of an additional oxidation peak above 0.9 V. The observed activation loss of the catalyst could be completely recovered as shown in ORR kinetic measurements (Figure 4 (C)). The full recovery was attributed to the weak adsorption of NO_x on platinum oxide in this potential region and easy removal of nitrate. This is in line with PEMFC single cell studies [61]. Consequently, the oxidative recovery procedure was identified to be an effective and fast recovery method after NO_x poisoning.

3.3.3 Recovery procedures for nitrogen oxide contamination

Recovery of performance losses by fuel cell operation in neat air are demonstrated by several studies. Mohtadi et al. reported full recovery at 600 mV, 70 °C and ambient pressure within 24 h after 12 h exposure of a fuel cell to 5 ppm NO_2 resulting in a performance loss of 55% [70]. Even if the recovery effect is referred by the authors to reductive recovery, the applied potential and the long recovery time suggests chemical desorption of NO_2. The study of Yang et al. has demonstrated performance loss up to 50 % caused by introduction of high NO_x concentration up to 1480 ppm using a mixture of 90% NO and 10% NO_2 for 1 h to an operating PEMFC. Thereby charge transfer losses and suppressed ORR due to NO_x adsorption were identified to be the main reason for the performance loss. Recovery during fuel cell operation was realized at 0.5 A cm^{-2}, 65 °C and 1.5 bar_{abs}. Cell recovery of 70 % was achieved within 3 min, but further recovery to 90% required 7 h. Full recovery could only be achieved using an additional purging step with nitrogen for 9 h. Thereby, it was demonstrated that slightly faster recovery is possible at ambient pressure. The recovery effect is attributed to NO_x oxidation and nitrate removal, even if the applied potentials during recovery are in the range of 0.6 to 0.7 V. Bétournay et al. have operated a PEMFC directly in mining environment with NO levels up to 42 ppm and NO_2 levels up to 10 ppm [93]. Without specifications of the operating conditions the complete recovery of the 40% performance loss was achieved by extended fuel cell operation in fresh air for 3 h. Garzon et al. exposed 5 ppm NO_x for 5 h to a PEMFC resulting in a performance loss of 15-20 % depending on the

Originally published on: *Journal of Power Sources 488 (2021) 229375*
DOI: 10.1016/j.jpowsour.2020.229375
https://doi.org/10.1016/j.jpowsour.2020.229375

applied relative humidity of the used air [67]. The operation in neat air for recovery was realized at 0.8 A cm^{-2}, 80 °C, and 2.1 bar_{abs}. 100 % cell performance recovery was achieved within 1 h referred to electrooxidation of NO_x at high potential combined with high water flow for nitrate removal.
The positive effect of potential cycling was shown by the study of Jing et al. [61], which examined the voltage loss of about 10% during 100 h fuel cell operation using air with 1 ppm NO_x (0.8 ppm NO_2 and 0.2 ppm NO). This demonstrated the slight performance decay using low concentration of NO_x impurities. CV measurements have confirmed NO_2 adsorption on the catalyst and ECSA reduction as the reason for the performance decay. It was additionally revealed that NO_x oxidation to nitrate takes place at 0.75 V under typical fuel cell operating conditions of 70°C and ambient pressure. This is significantly lower compared to 0.9 V in half cell measurements [95]. The potential cycling between 0.05 and 1.4 V during CV characterization resulted in fast and almost complete performance recovery.

Several studies have shown that recovery of performance losses caused by NO_x poisoning of the cathode catalyst is possible by fuel cell operation in NO_x-free air. Depending on NO_x poisoning extent, the operating conditions and the applied current density, this process can be very time consuming, which might be not feasible for system or even lab application. Half-cell CV measurements have shown that oxidation of NO_x to nitrate above 0.9 V accelerates the recovery and is superior to reductive removal. Additionally, it was demonstrated that this oxidation reaction can be realized in an operating fuel cell at lower cathode potentials of about 0.75 V. For fast and complete recovery, potential cycling under nitrogen proposes a reliable procedure for laboratory tests. For system application operating conditions at high cathode potential, e.g. idling operation could be a suitable procedure if balanced with the negative impact of potential catalyst and catalyst support oxidation. Nevertheless, this potential recovery strategy is not demonstrated in the literature so far.

3.4 Carbon oxide based contaminants

3.4.1 Reversible degradation caused by carbon oxides

Even low ppm concentrations of CO in the hydrogen feed can cause substantial and accumulating performance losses [51]. Thereby, low temperature, low humidity and high CO concentration enhance this effect, while the impact of pressure is small [101, 102]. CO impurities in the hydrogen could also affect the cathode catalyst as a result of CO crossover [103, 104], but the high oxidative environment of the cathode enables fast removal of adsorbed CO [105]. Consequently, the CO poisoning effect is an issue for the anode catalyst.
It is well known that CO binds strongly to the active sites of platinum catalysts, resulting in the reduction of surface active sites available for reactant conversion [51]. Cyclic CO-stripping voltammetry combined with either spectroscopic analysis of reaction species [106] and EIS [107] were used for kinetic analysis and for proving the link between CO poisoning and performance losses in the fuel cell. The strong adsorption of CO at platinum surfaces can be referred to two adsorption species which are governed by strong binding to substrate but also by strong lateral repulsion forces [108, 109]: (i) linear-absorbed CO blocking one adsorption site per CO molecule and (ii) bridge-bonded CO blocking two adsorption sites. These species are formed according to the following equations [110]:

(i) linear-absorbed CO:

$$\mathrm{CO} + \mathrm{Pt} \rightarrow \mathrm{Pt\text{-}CO_{ads}} \qquad (21)$$

Originally published on: *Journal of Power Sources 488 (2021) 229375*
DOI: 10.1016/j.jpowsour.2020.229375
https://doi.org/10.1016/j.jpowsour.2020.229375

(ii) bridge-bonded CO:

$$CO + 2\,Pt \rightarrow Pt_2{=}CO_{ads} \quad (22)$$

The impact of CO_2 to platinum catalyst activity is mainly referred to catalytic conversion to CO on platinum surfaces in a reverse water-gas shift reaction [111] and subsequent blocking of the catalytic surface sides of the platinum [112]:

$$2\,Pt + H_2 \rightarrow 2\,Pt\text{-}H_{ads} \quad (23)$$

$$CO_2 + 2\,Pt\text{-}H_{ads} \rightarrow Pt\text{-}CO_{ads} + H_2O + Pt \quad (24)$$

The CO poisoning caused by CO_2 presence at the anode can also be explained by a electrochemical reduction reaction according to [113]:

$$CO_2 + 2\,H^+ + 2\,e^- \rightarrow Pt\text{-}CO_{ads} + H_2O \quad (25)$$

Even if the mechanism for this poisoning source is still under discussion, it was demonstrated that low CO_2 concentrations of 1% are sufficient to produce enough CO to poison more than 50% of the platinum sites on a PEMFC anode [114]. CO_2 can enter the anode by permeation through the membrane from the cathode as shown in the literature [115, 116]. Consequently, CO poisoning of the anode catalyst can be a reason for significant performance losses in PEMFCs even if the hydrogen feed is free of CO. Recently, the aspect of CO poisoning is gaining increased attention again due to the development of ultra-low Pt-loaded anodes. High anode Pt loading of 0.4 mg_{Pt} cm^{-2} are only slowly effected by CO contamination and the performance loss is minor (about 5%), while current automotive SoA anode Pt-loading of 0.1 mg_{Pt} cm^{-2} results in a faster impact on performance showing severe performance losses of up to 30 % [117] Furthermore, the trend to use very thin membranes, which provides low ohmic resistance, increases CO_2 permeation from cathode to anode [118]. This can result in increased amount of adsorbed CO on the anode catalyst. Consequently, the topic of CO poisoning and recovery is of particular interest for automotive applications where such low anode Pt-loadings and thin membranes are established to be state of the art with targeted values below 0.05 mg_{Pt} cm^{-2} and 15 µm, respectively.

3.4.2 Requirements for performance loss recovery caused by carbon oxides

Recovery of performance losses caused by CO poisoning of the platinum catalyst requires CO oxidation to CO_2 as well as CO_2 desorption. Various studies have reported that the oxidation of CO to CO_2 may follow a chemical reaction, an electrochemical reaction or a combination of both. For the electrochemical oxidation of linear-adsorbed CO the following mechanism is generally accepted:

$$Pt + H_2O \rightarrow Pt\text{-}OH_{ads} + H^+ + e^- \quad E = 0.50\ V\ [51, 119] \quad (26)$$

$$Pt\text{-}CO_{ads} + Pt\text{-}OH_{ads} \rightarrow 2\,Pt + CO_2 + H^+ + e^- \quad E = 0.68\ V\ [47] \quad (27)$$

The mechanism for the electrochemical oxidation of bridge-bonded CO has been reported to be similar [110]:

$$Pt_2\text{-}CO_{ads} + H_2O \rightarrow 2\,Pt + CO_2 + 2H^+ + 2e^- \quad E = 0.40\ V\ [110] \quad (28)$$

Originally published on: *Journal of Power Sources 488 (2021) 229375*
DOI: 10.1016/j.jpowsour.2020.229375
https://doi.org/10.1016/j.jpowsour.2020.229375

The bridge-bonded CO is reported to be oxidized at lower potentials and CO oxidation as well as performance recovery can starts with these species but this is disputed as lateral interaction in the adsorption layer play an important role. However, it is undoubtful that the oxidation of linear-adsorbed CO which occurs at 0.68 V is required for full recovery of the Pt surfaces and removal of all adsorbed CO [110]. In both cases, water is considered to be the source of oxygen for the oxidation.

Under PEMFC conditions, CV and impedance studies at 80°C confirm that the potential of the CO oxidation peak is in the range of 0.6-0.7 V [107, 120]. For increasing CO coverages the CO_2 desorption peaks shifts to lower potentials [121] Even for CO tolerant catalysts, such as PtRu, the oxidation potential is reported to be at least 0.35 V [120]. Anodes of H_2/air fuel cells do not reach such high potentials during operation. In contrary, cathode potentials are typically high enough to easily remove CO by electro-oxidation.

The chemical mechanism for CO oxidation on the Pt surface involves oxygen which enters the anode by diffusing across the membrane from the cathode. It is reported that conversion of CO to CO_2 may occur as a catalytic surface redox mechanism [122]:

$$2\mathrm{Pt} + \mathrm{O_2} \leftrightarrow 2\mathrm{Pt\text{-}O_{ads}} \tag{29}$$

$$\mathrm{Pt\text{-}O_{ads}} + \mathrm{Pt\text{-}CO_{ads}} \rightarrow 2\mathrm{Pt} + \mathrm{CO_2} \tag{30}$$

3.4.3 Recovery procedures for carbon oxide contamination

A common method for the chemical oxidation of adsorbed CO on anode catalysts during PEMFC operation is the introduction of small amounts of air or oxygen into the fuel feed [51, 123]. A comprehensive literature overview regarding this external air bleeding technology is given in [116] and [124]. The majority of publications for air bleeding is focused on recovery or on steady-state operation of PEMFC using reformate as fuel and PtRu as CO-tolerant catalyst [101, 124, 125]. But the effect on pure Pt catalysts was also examined. The idea was introduced by Gottesfeld and Pafford in 1988 [123] showing that the cell performance of a Pt catalyst could be almost completely restored by injecting 2-5% oxygen to a hydrogen feed containing 100-500 ppm of CO. But the injection of air to the anode has also negative aspects. When oxygen is reduced on the anodic catalyst surface three competing reaction products can be formed: (i) chemical CO oxidation to CO_2, (ii) direct chemical reaction between oxygen and hydrogen to water and (iii) hydrogen peroxide formation which can lower the fuel conversion efficiency [123, 126]. Moreover, irreversible degradation occurs which include (i) membrane degradation [127] due to hydrogen peroxide formation [128, 129] and (ii) sintering of the catalyst due to the highly exothermic reaction between H_2 and O_2 [130]. Hence, it is important to minimize the amount of O_2 from the air bleed in order to reduce associated degradation effects. Perez et al. have shown that 75-80% recovery of the PEMFC performance using a hydrogen feed containing 20 ppm CO and a Pt anode catalyst can be achieves with air bleed levels below 2% and that increased hydrogen flow rate can facilitate the recovery process [116]. According to the model introduced by Zamel et al. performance recovery of 60% for 0.5% air bleeding ratio and of 70% for 1% were indicated for hydrogen containing up to 100 ppm CO [131]. Tingelöf et al. have reported full performance recovery at 80 ppm CO within about 4 min [132]. Thereby, an air bleed level of 0.5% per 10 ppm CO was required to achieve full recovery. Additionally, it was shown that the lower but clearly detectable poisoning effect of CO_2 can also be recovered using air bleed levels of 0.5%.

To avoid the efficiency losses and the negative impact on durability, the possibility of internal air bleeding was examined [105]. As for external air bleeding the adsorbed CO is oxidized at the Pt surface.

Originally published on: *Journal of Power Sources 488 (2021) 229375*
DOI: 10.1016/j.jpowsour.2020.229375
https://doi.org/10.1016/j.jpowsour.2020.229375

The required oxygen is not injected in the hydrogen stream, but is permeating from the cathode to the anode through the membrane [133]. The dissociative adsorption of oxygen is the rate-limiting step for this internal air bleeding (equation (29)). Jimenez et al. have shown that full recovery after poisoning with 72 ppm CO can be achieved within 15-30 minutes in fuel cell operation at room temperature and ambient pressure using neat hydrogen and oxygen without impact on lifetime [134]. Bender et al. [102] and Reshetenko et al. [135] provide detailed studies on the mechanisms of the CO oxidation during this performance recovery procedure under fuel cell operation by using different gases on the cathode and low CO concentration of 1-10 ppm on the anode. According to Bender et al. [102], the performance loss is caused by an increase in the anodic overpotential due to CO poisoning (Figure 5 (A)). This effect is enhanced for increasing CO concentration, lower temperature, lower humidity, and higher current. If the fuel cell is operated in neat hydrogen and air, the recovery rate is non-linear with a fast recovery of about 80-90 % in the first hour and a slow recovery of 5-15 h to 100%. The increased anode polarization by CO poisoning was further examined by variation of the cathode gas during recovery using hydrogen (hydrogen pump mode), air and pure oxygen. It was found that the performance recovery can be accelerated by increased oxygen crossover which enhances chemical CO oxidation (Figure 5 (B)). Increased oxygen concentration on the cathode, increased temperature and increased gas humidity are known to increase oxygen permeation across the membrane. [115, 136, 137]. Reshetenko et al. have investigated the involved CO oxidation mechanisms using EIS to prove contribution of electro-chemical CO oxidation by a pseudo-inductive loop at low frequency caused by surface relaxation [135]. In hydrogen pump mode with hydrogen as cathode gas and absence of oxygen, the adsorbed CO is only electrochemically oxidized, even if the anode overpotential of about 0.30 V is relatively low. This proves the statement that CO electrooxidation under fuel cell conditions is possible below the theoretical value of 0.6-0.7 V [131]. However, at low potentials the CO oxidation reaction rate is low and requires several hours. The electrochemical oxidation removes partially the CO until the overpotential is too low for further electrochemical reaction. The remaining CO cannot be removed, neither electrochemically nor chemically. Using air on the cathode enables full recovery within 10-15 hours by a combination of both oxidation mechanisms. At anode overpotentials of about 0.28 V electrochemical oxidation was detected and permeating oxygen from the air enables oxidation of remaining CO by chemical oxidation. The fastest recovery within 4-5 hours could be achieved using pure oxygen on the cathode. Thereby, the anode potential did not rise above 0.1 V and the authors demonstrated that the potential did not vary significantly over the active area. Consequently, electrochemical oxidation was not observed and the CO was oxidized only chemically under these conditions.

Originally published on: *Journal of Power Sources 488 (2021) 229375*
DOI: 10.1016/j.jpowsour.2020.229375
https://doi.org/10.1016/j.jpowsour.2020.229375

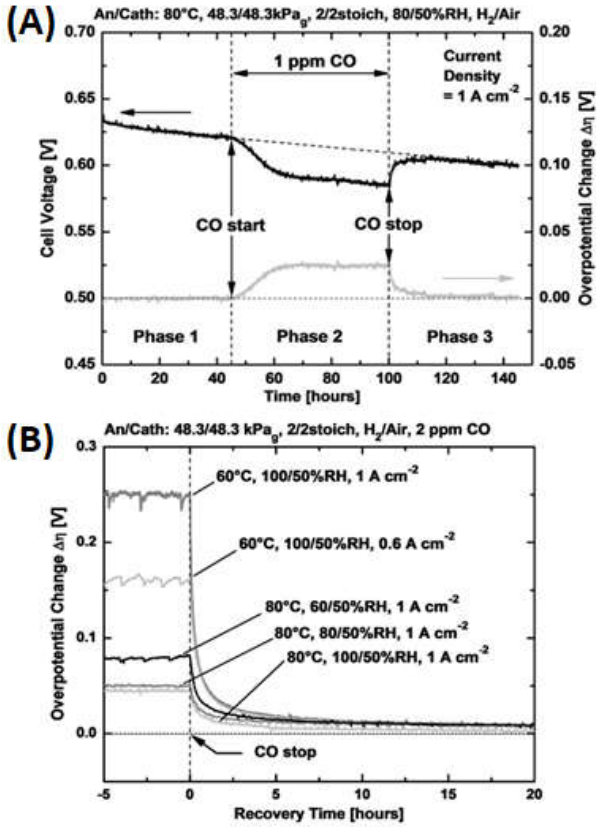

Figure 5: (A) Cell voltage response during exposure to 1 ppm CO in the H_2 fuel and recovery in neat H_2 within 5-15 h as well as (B) the impact of operating conditions on the recovery effect, reprinted from [102] with permission from Elsevier.

Oxidation of the remaining CO traces on the catalyst requires the presence of oxygen and is a slow process, which depends on the concentration of oxygen at the anode catalyst. For internal air bleeding, this concentration is depending on the rate of O_2 permeation through the membrane. The permeation rate of oxygen N_{O2} can be expressed as [122]:

$$N_{O_2} = K \cdot D \cdot p_{O_2}/L \tag{31}$$

with the Henry's law constant K, the diffusion coefficient D of O_2 in the membrane, the membrane thickness L, and the partial oxygen pressure in the cathode p_{O2}. Consequently, permeation rate and thus improved chemical CO oxidation on the anode can be achieved by: (i) lowering the membrane thickness L [105, 122], (ii) increasing p_{O2} by increasing the pressure in the cathode compartment [105, 122] or by increasing oxygen concentration in the cathode feed [102, 122, 135], and (iii) increasing the diffusion coefficient D of O_2 in the membrane, realized by increasing temperature [102, 105] or humidity [102]. The combination of different advantageous conditions for increased oxygen permeation has been shown to enable fast recovery of performance losses caused by CO poisoning of the anode catalyst during fuel cell operation [103, 104, 138]. Zhang et al. have demonstrated that full recovery is possible within 2 minutes using the combination of thin membranes, pure oxygen and increased pressure on the cathode. However, using pure oxygen for performance recovery is not applicable to systems and raises safety issues. Moreover, non-uniform oxygen diffusion over the active area of a MEA may result in remaining local CO poisoning [116].

Originally published on: *Journal of Power Sources 488 (2021) 229375*
DOI: 10.1016/j.jpowsour.2020.229375
https://doi.org/10.1016/j.jpowsour.2020.229375

A method to increase anode overpotential by increasing current density to enable CO oxidation on the anode is the so-called pulsing recovery technique. It is based on "self-oxidation" or "sustained potential oscillation" using PtRu anode catalysts and reformate fuel [139]. Using CO levels of 100 ppm and higher, an oscillating phenomenon was observed in PEMFCs operated at constant current: (i) CO adsorbs on the catalyst until the surface is almost completely blocked, (ii) in order to sustain the applied current, the anode becomes increasingly polarized to a higher potential accelerating the electrochemical oxidation of adsorbed CO on the catalyst surface. At certain overpotential, the CO oxidation rate exceeds the rate of CO adsorption and the surface coverage of CO drops. Accordingly, the anode overpotential drops quickly and the process starts again.
This self-oxidation mechanism does not take place for low CO concentrations and for Pt catalysts. In both cases, the anodic overpotential does not reach the threshold above which the CO oxidation rate exceeds the CO adsorption rate. Nevertheless CO oxidation on Pt can occur before this threshold at lower potential of about 0.3 V as shown before [135]. Consequently, performance recovery after CO poisoning can also be triggered by increasing the anodic overpotential during fuel cell operation. The pulsing recovery technique applies short pulses of high current to apply these overpotentials. Thereby, the current has to be adapted for each electrode to enable high enough overpotential for CO electro-oxidation and pulses shorter than 1 s are sufficient [131, 140]. It was demonstrated in hydrogen pump mode that this technology can also be applied to Pt catalysts to evaluate the anode effect separated from the ORR effects [131, 141], but high anodic overpotentials are required. Jimenez et al. have shown that this technique can fully recover performance losses due to CO poisoning during fuel cell operation using 50 ppm CO in the hydrogen feed [134]. The applied current pulses resulted in negative cell voltages and cell reversal which may be detrimental for cell durability. The cell potential control is challenging for this technique. This limits the applicability of this technique to fuel cell stacks and requires special equipment for control of individual single cell voltages [131].

In general, there are two mechanisms for performance recovery after CO poisoning, chemical and electrochemical oxidation of the adsorbed CO. Electrochemical oxidation can be triggered by high anode potentials and chemical oxidation requires oxygen at the anode. Due to safety requirements and complex control systems, external air bleeding is not the method of choice to provide oxygen to the anode. But internal air bleeding by oxygen diffusion through the membrane can be used for both, system and laboratory applications. Thereby, conditions with increased oxygen permeation are beneficial for recovery. This recovery effect can be assisted by increased anode potential at high current density. In summary, the best procedure for performance recovery after CO poisoning of the anode is high current fuel cell operation under high temperature, high pressure and high humidity. For these conditions, the high load operation and the use of thin membranes enable fast performance recovery after CO poisoning without interruption of the fuel cell operation and represent typical automotive operating conditions [18].

4 Ionomer and membrane degradation

4.1 Ionomer and membrane structure changes

4.1.1 Reversible ionomer structure changes

Changes of ionic conductivity of the electrodes is usually evaluated by AC impedance which may provide indication for ionomer degradation in the electrodes [12]. However, the discrimination

Originally published on: *Journal of Power Sources 488 (2021) 229375*
DOI: 10.1016/j.jpowsour.2020.229375
https://doi.org/10.1016/j.jpowsour.2020.229375

between reversible and irreversible ionomer changes in the literature is very scarce. Explicit reversible performance losses due to ionomer structure changes in the electrodes are reported at both dry and humid operation conditions [142, 143]. The degradation of ionomer in the membrane is irreversible and can be monitored by measuring hydrogen cross-over which is one of main indicators for membrane's state-of-health [12]. Nevertheless, small pin holes formed due to radical attack, which are irreversible defects, can be temporarily sealed by membrane swelling at highly humid conditions [144]. Jomori et al. [142] report a decrease of the activity of cathode catalyst layer after low humidity operation and a recovery after subsequent high humidity operation at the time scale of hours. The reason for this relatively slow change is explained by changes of the ionomer structure in the cathode catalyst layer resulting in an adsorption of ionomer on the platinum catalyst surface. The authors paid special attention to discriminate between effects due to ionomer changes and effects of PtO_x formation by applying specific test procedures to keep PtO_x formation constant. Possible models are proposed which consider increase of oxygen transport resistance though the ionomer due to adsorption of sulfonate groups at the Pt particles at low relative humidity.

Langlois et al. [143] also identified ionomer structure changes as one mechanism being responsible for reversible degradation in potential cycling conditions in H_2/N_2 atmosphere. It is noted, that the detrimental "ionomer relaxation", which can be recovered by exposure to dry N_2 at high temperatures, was reported to occur in highly humid conditions and not in dry conditions. This effect was investigated by AFM analysis of the ionomer exposed to hot water vapor. The data shows that ionomer structure changes increase with increasing relative humidity (RH) and temperature as shown in *Figure 6*. Apparently, ionomer structure changes occur much faster at high RH compares to low RH. Additionally, the impact of the potential cycling on performance decay depends on Pt-loading and the catalyst to carbon ratio of the electrode. The lower the Pt-loading, the higher is the observed performance degradation. Moreover, the lower the Pt-loading the greater is the relative ECSA loss which was clearly demonstrated at 20 wt% Pt:C ratio, i.e. the effect of Pt dissolution is greater when the absolute amount of Pt is lower [143]. The observation of (i) a correlation between ECSA loss and performance loss in the kinetic region of the polarization curve and (ii) a lack of a corresponding correlation at high current density suggests that another non-kinetic parameter is limiting performance in the mass-transport region. A possible explanation is given by ionomer structure changes that seem to play a major role at high current densities. This hypothesis is supported by: (i) performance losses at high current density that do not correlate with kinetic parameters, (ii) ionomer structure changes observed with AFM (detrimental relaxation at high RH) and (iii) the changes in porosity of the CL after performance recovery process (dry N_2 exposure at high temperature) which are explained by suppressing of ionomer relaxation that leads to tightening of mesopores of the catalyst layer.

Originally published on: *Journal of Power Sources 488 (2021) 229375*
DOI: 10.1016/j.jpowsour.2020.229375
https://doi.org/10.1016/j.jpowsour.2020.229375

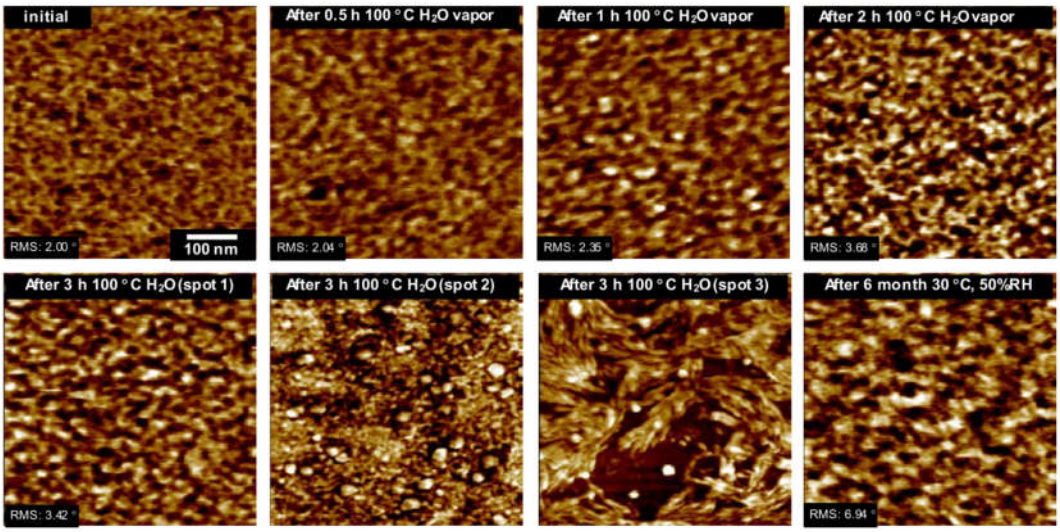

Figure 6: Ionomer (bright areas) structure changes at different humidity observed using AFM images (500 nm size) of Nafion film during water vapor exposure, reprinted from [143] with permission from Elsevier.

4.1.2 Recovery of reversible ionomer structure changes

As reported by Jomori et al. [142] low RH operation leads to reversible degradation due to ionomer adsorption on Pt surface that is recovered by high RH operation and certain voltage cycling. Furthermore, it is suggested that the changes of the ionomer adsorption structure at dry conditions result in dense ionomer layers that increase local O_2 transport resistance [145]. Recovery of associated activation losses and increase of oxygen transport resistance due to ionomer structure change occurs at the time scale of hours. It was demonstrated that low potentials and highly humid or even condensing conditions result in improved recovery effect. Potentials below 0.2 V are required for best recovery at 95% in the reported experiments. The requirement of low potential seems to be a result of sulfonate desorption below the point of zero charge. To fully recover the reversible losses under these conditions a hold time of 8h is necessary [142]. Such a long recovery time is hardly applicable in real applications. Hence, a mitigation strategy avoiding prolonged dry operation is preferred. This aspect should be considered when defining operating conditions. For instance, in the JRC EU Harmonised Test Protocols for PEMFC single cells [14] cathode humidity was defined as 30 % RH which may lead to reversible ionomer structure degradation upon drying.

According to Langlois et al. [143] the ionomer structure relaxation observed at high RH can be recovered by purging the cell with dry nitrogen at high temperatures of 90-120 °C (thermal treatment). This treatment significantly reduces reversible degradation at high RH operation conditions and extends the MEA lifetime by factor 5. Thereby, the extended duration of the dry hot nitrogen treatment for several hours also positively affects the recovery step. When a dry air flow was applied instead of nitrogen, the efficiency of the recovery was significantly lower due to other effects related to increasing cathode potential. Interestingly, the recovery procedure also significantly reduces ECSA loss which is explained by local concentration changes of the ionomer at the Pt particles affecting their dissolution and migration properties.

Membrane pinholes and micro cracks occurring due to radical formation and mechanical stress upon long term operation lead to gas crossover causing mixed potentials at the electrodes. Generally, H_2 cross over increases with increasing operating pressure and increasing operation temperature. The

Originally published on: *Journal of Power Sources 488 (2021) 229375*
DOI: 10.1016/j.jpowsour.2020.229375
https://doi.org/10.1016/j.jpowsour.2020.229375

dependence of the H_2 crossover rate of an intact membrane on RH is less evident [146]. For defective membranes, however, RH can have a very strong effect on H_2 cross over. As reported by Kreitmeier et al. [144], liquid product water can be used to seal these membrane defects and mitigate gas crossover. On the contrary, drying condition can result in membrane shrinking, which may enlarge micro cracks and increase the gas crossover [147]. Consequently, a recovery procedure for membrane effects could include an increase of the cell humidity and a decrease of the mechanical stress applied to the membrane. The recovery of microcracks by soaking the MEA at high RH conditions is only a temporary solution due to the irreversible nature of this degradation effect. When returning to regular fuel cell operations the performance drop due to H_2 cross over becomes evident after several hours [13].

4.1.3 Summary and recovery procedures of ionomer degradation

Different studies considering reversible ionomer degradation are published and explain reversible performance losses by detrimental ionomer structure changes in the catalyst layer. Two different effects of ionomer changes at nano-scale and meso-scale are proposed which occur at dry and at humid conditions, respectively. Inferior ionomer arrangement in the vicinity of platinum particles or increases oxygen transport resistance through the ionomer film (changes at nm-scale) occur at time scale of hours at dry conditions and are caused by absorption of ionomer sulfonate groups on Pt surface [142]. These losses could be recovered by operation at low electrode potentials at high RH. In contrast, changes referred as “ionomer relaxation” lead to tightening of meso-pores (changes at <20 nm-scale) occur in humid conditions and are recoverable by exposure to dry gas at high temperature for about 1 h [143]. These are opposite effects indication that prolonged humid as well as prolonged dry conditions are detrimental. However, the possible explanations are speculative and the details of the ionomer structure changes at the nano-scale are not well understood. Hence, providing specific detailed solutions is difficult and only phenomenological advice can be provided. A common observation is that performance losses and performance recovery addressed to ionomer structure changes occur at the time scale of hours. Consequently, a rapid recovery procedure to be regularly applied is not possible since the procedures require a prolonged interruption of system operation. For an automotive system, this could be realized during shut-down periods. Especially, the thermal treatment of the membrane seems to be very promising to significantly extend fuel cell lifetime and providing low potentials during shut-down periods could recover occurring performance losses during fuel cell operations.

4.2 NH_3/NH_4^+ and salt contamination of ionomer

4.2.1 Performance loss due to ammonia and salt contaminations

The properties of the ionomer in the catalyst layers and in the membrane is influenced by ammonia and salt cations, such as Na^+, Ca^{2+} or Mg^{2+}, in various ways leading to mainly ohmic and kinetic performance losses [67, 148, 149]. For ammonia, the general observation is that the performance losses increase with increasing NH_3 concentration. Mechanisms of performance losses due to NH_3 contamination, well summarized in [148], are: (i) decrease of ionomer conductivity by NH_4^+, (ii) adsorption of NH_3 in the anode and cathode catalyst layer affecting the ionomer/catalyst contact and indirectly reducing HOR and ORR kinetics [99, 100, 150].

In the paper by Gerzon et al. [67] low concentration of NH_3 of 1 ppm leads mainly to ohmic losses which are high during the first 160 h of operation. For the subsequent operation period up to 400 h no further performance drop is visible. At increased NH_3 concentration of 48 ppm, on the other hand,

Originally published on: *Journal of Power Sources 488 (2021) 229375*
DOI: 10.1016/j.jpowsour.2020.229375
https://doi.org/10.1016/j.jpowsour.2020.229375

dramatic losses in the kinetic region of the polarization curve as well as some minor ohmic losses are visible already after 1 h of operation. Similarly, the negative effect of Mg^{2+} contamination on ohmic resistance of the PEMFC due to ion exchange between Mg^{2+} and the proton of sulfonic acid groups in the membrane increases with Mg^{2+} concentration [151].

In their detailed study, Gomez et al. [148] determined the performance losses due to NH_3 (up to 200 ppm concentration) of the individual MEA components. Corresponding ionomer resistance measurements indicate that largest contributions are due to kinetic losses via indirect catalyst deactivation by affecting ionomer/catalyst interface, followed by ohmic losses due to ionomer in the catalyst layers, and followed ohmic losses due to the ionomer of the membrane. The catalyst deactivation is demonstrated by ECSA loss seems attributed to reduced accessibility of active sites due to reduced ionomer/catalyst interface and is not correlated with actual ORR activity. It is worth to mention that the results suggest an irreversible part of ionomer degradation due to NH_3 which is addressed to ionomer structure changes leading to a permanent loss of the contact between ionomer in the catalyst layer and the Pt catalyst particles and Pt dissolution [148].

According to Hongsirikarn et al. [149] metal cation contamination (Na^+, Ca^{2+}, Fe^{3+}) leads to even stronger reduction of membrane conductivity than NH_3 contamination. Moreover, the conductivity change of the membrane contaminated by metal cations shows a strong temperature dependence; while at room temperature (liquid water) the conductivity due to cation contaminations was reduced by factor 12, at 80°C (humidified gas) the conductivity was reduced by 120 times.

4.2.2 Recovery of ammonia and salt contaminations

The recovery of NH_3 contamination of membrane reported by Gerzon et al. [67] occurs via oxidation to ammonium and dissolution into product water. Thereby the recovery time decreases with increased current density, pointing at the importance of the presence of product water for the recovery procedure. While less than 5 h recovery time is needed at 0.9 A cm^{-2}, the recovery time equals to 35 h at 0.2 A cm^{-2}. The positive effect of water produced at high current density on membrane conductivity during NH_3 recovery is also reported by Gomez et al. [148]. The effect of high current density is particularly beneficial if NH_3 is present at the cathode side. In case of anodic NH_3 contamination neat hydrogen operation is considered adequate recovery procedure. However, there is a partial irreversible performance loss related to ECSA loss that cannot be recovered. A further observation shows that short exposure to high NH_3 concentrations can be recovered more easily that prolonged NH_3 exposure at low concentrations.

The ion exchange reaction to replace metallic cation contaminations (such as Na^+, Ca^{2+} or Mg^{2+}) in the ionomer by H^+ usually requires boiling in acid which cannot be performed as an operando procedure and is therefore considered as non-recoverable.

4.2.3 Recommendation on mitigation of ammonia and cation contaminations

Metal cation contamination in ionomers mainly leads to irreversible increase of ohmic losses of the membrane. Therefore, the mitigation of these contaminants has to be addressed when gas purity is considered. Trace contamination by NH_3, on the other hand, is recoverable by neat hydrogen operation at high current density leading to liquid water formation at the cathode. These conditions can be easily implemented in a PEMFC system operation strategy. However, prolonged exposures to NH_3 in the order of tens of hours lead to irreversible catalyst layer changes and should be avoided.

Originally published on: *Journal of Power Sources 488 (2021) 229375*
DOI: 10.1016/j.jpowsour.2020.229375
https://doi.org/10.1016/j.jpowsour.2020.229375

5 Catalyst support degradation

5.1 Reversible catalyst support degradation

One of the major reasons for performances losses in PEMFC is carbon corrosion as the catalyst material, Pt nanoparticles and their alloys, are usually dispersed on porous carbon black (e.g., Vulcan XC-72). There has been much effort to understand the electrochemical corrosion behavior of carbon materials in the PEMFC working conditions. It is widely accepted that the carbon corrosion is a result of carbon oxidation reaction in the cathode of the fuel cells under following conditions: (i) local fuel starvation, (ii) start up and shut-down conditions, (iii) great permeability of oxygen through the membrane [152-157]. Nowadays, carbon corrosion under operating conditions is usually considered to be of lower importance. Whereas the high potentials at the cathode during fuel cell start-up and shut-down can result in accelerate carbon corrosion. Cathode potentials significantly higher than 1 V can occur due to hydrogen/air fronts caused by gas exchange processes in these phases [158]. During the reaction it is suggested to form a range of oxide species on the carbon surface at voltage above 0.3 V (RHE) in the presence of Pt, such as quinones/hydroquinones, lactones, carboxylates etc. [159-161]. These oxygen-containing groups are finally oxidized to gaseous CO_2, which has been proven by XPS [162, 163], gas chromatography [164], and IR spectroscopy [165] and non-dispersive infra-red (NDIR) [166]. The electrochemical oxidation of carbon generally proceeds as shown in Figure 7 (A) [45, 167-174].

The carbon corrosion rate is determined by many functions including temperature, electrochemical potential, water partial pressure and even the morphology of the carbon material [175, 176]. As a result of carbon corrosion, the porosity and thickness of the catalyst layer are reduced, and the carbon surface become more hydrophilic which increases the risk of electrode flooding [177, 178]. The catalyst utilization decreases because of particle agglomeration. At moderate PEMFC conditions, the accumulation of surface oxide species promotes the wetting of carbon support and further enhances the carbon corrosion [178-180]. In a corroded cell both kinetic and mass transfer resistance are reported to increase dramatically after certain corrosion ASTs, which lead to reduced efficiency and increased internal heat generation and thermal gradients [178].

In the carbon oxidation process, only the initial reactions of the formation of hydroxyl groups from defect sides in the carbon structure and of the subsequent oxidation to carbonyl groups are reported to be reversible [47, 153, 157, 168], as shown in Figure 7 (A). With the presence of Pt nanoparticles at electrode potential over 0.6 V, oxygenated species resulting from water splitting on Pt facilitate the removal of carbon surface oxide species and speed up the kinetics of carbon corrosion [181, 182]. It is known that carbon corrosion takes place at high electrode potentials. Especially during the fuel starvation and start-up/shut-down phases of a fuel cell, local cathode potential can reach up to 1.4 V [164, 166, 183], resulting in pronounced carbon corrosion, detachment of the Pt nanocrystallites, and massive ECSA losses [174]. Therefore, the use of potential cycling in the range of 0.4 - 1.4 V is a commonly accepted method to investigate the mechanism of carbon corrosion.

Originally published on: *Journal of Power Sources 488 (2021) 229375*
DOI: 10.1016/j.jpowsour.2020.229375
https://doi.org/10.1016/j.jpowsour.2020.229375

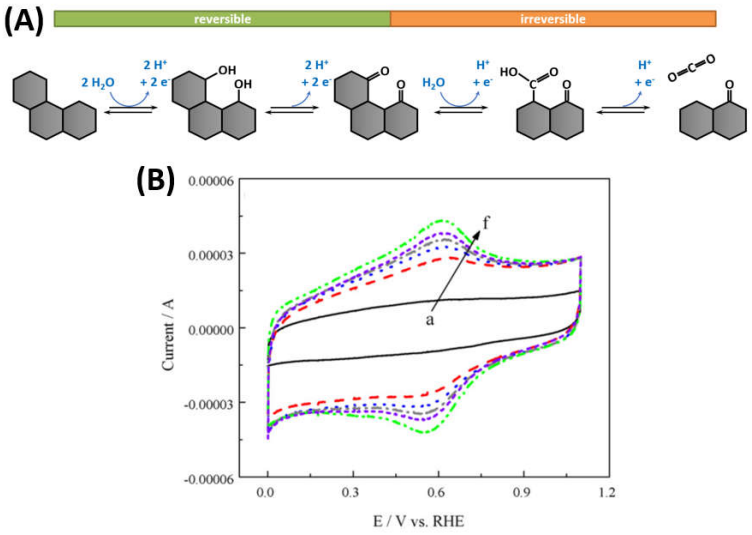

Figure 7: (A) Reversible and irreversible oxidation reactions of the carbon support material. (B) Cyclic voltammetry of a carbon support after electrochemical oxidation, reprinted from [167] with permission from Elsevier.

As shown in Figure 7 (B) [167], a carbon-based electrode was characterized with CV before and after the stressing test. The obvious reversible current peak around 0.6 V in each CV curve after stressing condition is attributed to the hydroquinone-quinone (HQ/Q) redox couple, which was produced during the carbon oxidation. The charge in the HQ/Q region can be used to calculate the oxidation degree of the carbon support [170, 184-186]. The symmetrical electrical charge for reduction and oxidation is a sign of reversibility of the reaction. However, Zhao's group did a similar CV test using a carbon supported Pt catalyst and with OCV as stressing factor [165]. The electrical charge under the reduction peak decreased which suggested that the hydroquinone groups present on the carbon surface were irreversibly oxidized.
In contrary, it is widely accepted that the ring opening reaction of the graphitic carbon structure under formation of carboxyl groups and the evolution of CO_2 is irreversible and cannot be recovered [47, 153, 157, 168].

5.2 Mitigation of catalyst support degradation

In a PEMFC, the working environment in the cathode composing of high oxygen concentration, high electrode potential (> 0.6 V), low pH, high temperature and high humidity is harsh for the support material to resist corrosion. The ultimate solution to develop corrosion resistant catalyst support by (i) modification of carbon black such as nitrogen-doping [187, 188], (ii) utilization of novel carbon materials like carbon nanotubes [189, 190], (iii) reduce the pore size and increase the hydrophobic property [180]. Besides, many researchers proposed system strategies to reduce the effect of carbon corrosion. To eliminate the local fuel starvation a fuel-cycle loop can be used to provide a high velocity through the anode [191, 192]. For a fuel cell stack, a good design of fuel manifold guarantees the uniform distribution of hydrogen in order to avoid negative voltage in single cell under high fuel utilization and fast load transients [193, 194]. To mitigate carbon corrosion during start up and shut-down conditions, UTC Power proposed to use an extra dummy load as a voltage-limitation device to keep the fuel cell voltage at a safe level. In this way the stack voltage was steady even after 12000 start/stop cycles [166]. Choo et al. [48] published a patent aimed to recover the performance loss of

Originally published on: *Journal of Power Sources 488 (2021) 229375*
DOI: 10.1016/j.jpowsour.2020.229375
https://doi.org/10.1016/j.jpowsour.2020.229375

fuel cell stack with hydrogen pumping, which reduce the carbon oxide by spillover of the hydrogen from platinum to carbon. Thus, the hydrophobicity of the carbon support in the cathode may be recovered and the performance of the fuel cell stack could increase due to the improved water management. However, in a follow-up paper from the same group [47], it is demonstrated that the ratio of C-C aromatic bonding on carbon surface did not show remarkable change before and after hydrogen pumping. The irreversible reaction was confirmed to be predominant.

5.3 Recovery procedures for catalyst support degradation

Generally, there is a range of contributions, which focus on the understanding of the mechanism of carbon corrosion process. However, only few of work mentioned that the performance loss during the carbon corrosion might be recovered. Besides that, none of them in the published literature developed or proposed effective recovery procedure against the reversible performance degradation caused by carbon corrosion.

6 Water management phenomena

6.1 Reversible performance losses caused by water phenomena

A proper water management is of great importance for the fuel cell's long-term performance. The issue of water management in the fuel cell has been extensively studied in the past [195-199]. PEMFCs always undergo dynamic operating conditions during the lifetime, which results in a range of water's generation, elimination, and transport phenomena. The relative humidity is one of the most important operating parameters to take an effect to the water management in the fuel cell. From Figure 8 (A), it is clearly to see that certain relative humidity is critical to obtain a high fuel cell performance. Especially the relative humidity in the cathode is the main parameter controlling the performance stability [200, 201]. Except the water from the humidifying device, water is also yielded as a product of ORR in the three-phase boundary interface [202]. The accumulated liquid water in the electrodes gas porosities must be transported away from the catalyst layer by evaporation, water–vapor diffusion and capillary transport through the GDL [203, 204]. Otherwise, the excess liquid water can occupy the surface of the catalyst and/or block the porous path for oxygen in the electrode, resulting in dramatic performance loss which is called flooding. On the other hand, water is crucial to guarantee the high proton conductivity in the ionomeric phase [202, 205]. The widely used electrolyte and electrode material is supported by sulfonic acid group (HSO_3), which constitutes the ionomer structure [206, 207]. Only in wet conditions the sulfonic acid bond can be dissociated and the protons can move from an acid group to another, which enables the migration and conductivity of protons [203, 208]. Besides, the reduced ionic conductivity of the membrane can hinder the access of protons to the catalyst surface, lead to obviously increased activation polarization, furthermore, even mechanical cracks and delamination of the membrane [209]. It is reported that a fully hydrated membrane can guarantee up to 300 times higher conductivity than a dry one [210]. The dehydration of membrane can be generally attributed to: (i) insufficient humidified or dry reactant gas flow, (ii) the operating conditions cannot provide enough water for the membrane, e.g. at idling condition or low current density, (iii) electro-osmotic drag prevails back diffusion, especially at high current density [211]. The liquid water in the GDL and flow channels tend to accumulate and block the gas path only after the complete saturation of the gas vapor in the electrodes, because both the capillary mechanism within the GDL and the drag force exerted by the convective flow in the channels are slower than the evaporation and water vapor

Originally published on: *Journal of Power Sources 488 (2021) 229375*
DOI: 10.1016/j.jpowsour.2020.229375
https://doi.org/10.1016/j.jpowsour.2020.229375

transport [213, 214]. For fuel cell stack it is especially a challenge to supervise and control the water management in each cell to keep a stable and homogeneous humidity distribution [215, 216].

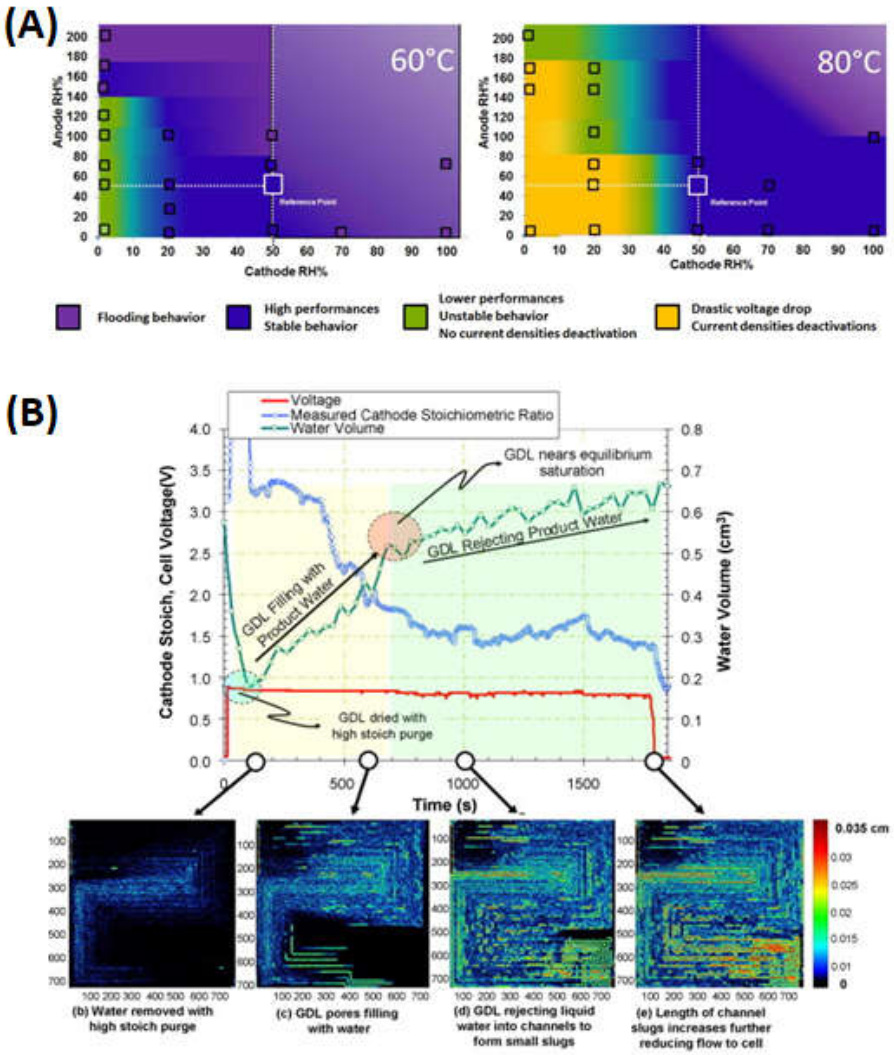

Figure 8: (A) Relation between relative humidity and cell performance stability respectively cell flooding, reprinted from open access article [200] under the terms of the Creative Commons Attribution 4.0 License. (B) Cathode behavior after removal of liquid water by gas purging, reprinted from [217] with permission from Elsevier.

6.2 Performance loss recovery caused by water management

Generally, the performance loss caused by local water flooding and temporary membrane dehydration could be recovered by adjusting the operating parameters of the fuel cell. Shut-down and restart phases during fuel cells operation may provide the first clue to the researchers about the recoverable and irrecoverable performance. Qi et al. [218] called the phenomenon saw-tooth, as the fuel cell's performance increased after the shut-down and restart during stress tests. Some hypotheses were investigated to result in this pattern. Through several potential cycling tests, the contribution of catalyst oxidation state change and surface contaminants cleansing was confirmed to be negligible. After a flooding simulating test, the removal of excess water from the fuel cell was confirmed to make significant contributions to the recovered performance during the shut-down and restart process. The

Originally published on: *Journal of Power Sources 488 (2021) 229375*
DOI: 10.1016/j.jpowsour.2020.229375
https://doi.org/10.1016/j.jpowsour.2020.229375

excessive water was purged out and the water in the cell was redistributed during the OCV conditions. Similar results were also reported during MEA ageing tests [219].

Cathode gas purge was utilized by many researchers as an effective recovery procedure to resolve the flooding problems during fuel cell operation [9, 46, 217, 220-222]. According to Owejan et al. [217] the retained water in the gas diffusion layer reached initially a saturation fraction and then accumulated in the flow channels. The performance loss resulting from the dynamically flow-channel slug could be recovered by increasing the flow rate of air. The transient correlation of purging process was captured and quantified by the in-situ neutron radiography in Figure 8 (B). Unlike the instant recover of performance, the liquid water content in the gas diffusion layer decreased slowly, indicating that GDL liquid water accumulation was not the main contributor to the mass transport limitation. On the other hand, gas purge is not the most effective method to recover the fuel cell performance loss induced by certain operating scenarios. For example, the recoverable loss after long term open-circuit aging tests mainly owes to the platinum oxidation (section 2) and catalyst contamination (section 3). Gas purging which helped with water removal and catalyst surface flushing, was still less effective than the recovery procedure with potential cycling [221].

Stumper et al. [209] reported an instant performance recovery upon a switch-back from dry gas to humidified gas operation, which was derived from the rehydration of the membrane. With the segmented cell, the ohmic resistance in the oxidant inlet was higher relative to the other segments after the recovery. Besides, the inlet segment recovered slower than other parts of the cell, which implied that the membrane rehydration was strongly affected by water production. Cho's group investigated the transient behavior of the membrane rehydration and confirmed this theory in-depth [223]. Under a sudden increase of load, the membrane dehydrated, which was then improved due to the supply of humidified gas, internal hydration from electroosmotic drag and back diffusion.

The recovery procedure adjusting the water management in the fuel cell was frequently taken as an important part of the Fault Tolerant Control Strategy (FTCS). After faults were detected thanks to physical and analytical redundancy, the remedial actions would be undertaken. In the work of Lebreton et al. [224], four successive flooding and recoveries steps were recognized and conducted respectively. The cathode pressure drops reacted instantaneously to gas flow modification, while voltage declined slower, presumably because of diffusion phenomenon. Therefore, both the fact of pressure drop increasing and voltage decreasing were expected to be taken as diagnose signals of flooding and gas flow modifications were identified as applicable recovery procedure [225].

Summarized, most recovery procedures to improve the water management of the fuel cell were focused on the water removal and flooding prevention, mainly included gas purging and humidity regulation. For the purpose of water removal there were other extra devices utilized in the literature [226, 227], like electroosmotic pump and sequential exhausting device attached to the fuel cell stack. However, in consideration of the auxiliary power and size, these devices are only recommended for laboratory use. To optimize the recovery methods, more work should be in progress, evaluating the step characteristics and corresponding impact, like the duration and velocity of the gas purging. On the other hand, water balance during the fuel cell operation is an accumulative complex mechanism, which always implicates other fuel cell components [228, 229]. Pivac et al. confirmed that the reversible performance after frequent shut-down operations was attributed not only to the accumulated water but also to the formation of platinum oxides [230]. Recovery procedures aiming to

Originally published on: *Journal of Power Sources 488 (2021) 229375*
DOI: 10.1016/j.jpowsour.2020.229375
https://doi.org/10.1016/j.jpowsour.2020.229375

rebalance the water may change the hydration of the membrane at the same time, which should also be considered during the evaluating. Gazdzicki et al. [13] have observed that the high recovery of reversible performance losses obtained by a shut-down recovery procedure seems to be the result of different effects but the highest impact on the performance recovery of reversible voltage losses is water rebalancing of the cell. Additionally, the presence of contaminants at the anode demonstrated a minor but significant impact. The sum of the effects due to purging the anode with air and temporarily reducing cell temperature is able to explain the most of the reversible losses. This combination of high anode potential for contaminant removal and reduced mechanical stress to the membrane leads, at least for high current densities, to the full recovery effect achieved by the shut-down recovery procedure. Under dry operation conditions temperature drop to condensate water is an effective recovery procedure whereas at humid operation condition gas purging is essential. For the latter case material ageing leading to hydrophobicity loss is an accelerating factor [231].

7 Conclusion

Reversible performance losses in polymer electrolyte membrane fuel cells and available recovery strategies for the different degradation mechanisms are summarized in this review. Table 3 shows an overview of the involved degradation processes and summarizes the requirements and the procedures examined in the literature for the recovery of reversible performance losses.

Originally published on: *Journal of Power Sources 488 (2021) 229375*
DOI: 10.1016/j.jpowsour.2020.229375
https://doi.org/10.1016/j.jpowsour.2020.229375

Table 3: Overview of reversible degradation mechanisms and recovery procedures for PEMFC

Reversible degradation mechanism	Cause for performance loss	Recovery strategy	Recovery mechanism	Electrode potential vs. RHE	Recovery procedures	References
Pt oxidation	PtO_x ($-OH$,$-O$,$-O_2$)	PtO_x reduction	$Pt\text{-}O_2 + Pt + 2H^+ + 2e^- \rightarrow 2Pt\text{-}OH_{ads}$ $Pt\text{-}O + H^+ + e^- \rightarrow Pt\text{-}OH_{ads}$ $Pt\text{-}OH_{ads} + H^+ + e^- \rightarrow Pt + H_2O$	< 0.63 V [22] < 1.145 V [22] < 0.65 V [22]	Cyclic voltammetry in H_2/N_2 Low potential pulses in H_2/N_2 High current / low potential in H_2/air H_2 atmosphere on cathode Hydrogen pump operation	[26, 27, 34-38, 42] [43] [37, 39, 44] [37, 45, 46, 47] [47, 48]
Adsorbed sulfur species	Pt···S	Pt-S oxidation and sulfate desorption	$Pt\text{-}S_{ads} + 4H_2O \rightarrow Pt\text{-}SO_4^{2-}{}_{ads} + 8H^+ + 6e^-$ $Pt\text{-}SO_4^{2-}{}_{ads} \rightarrow Pt + SO_4^{2-}$	> 0.9-1.3 V [47] < 0.17 V [86]	Cyclic voltammetry in H_2/N_2 Cyclic voltammetry in H_2/in-situ N_2 High and low potential pulses in H_2/N_2 OCV phases in H2/air	[62, 70, 71, 73] [21] [74] [73]
Adsorbed sulfate and sulfonate	$Pt\cdots SO_4^{2-}$	Sulfate or sulfonate desorption	$Pt\text{-}SO_4^{2-}{}_{ads} \rightarrow Pt + SO_4^{2-}$	< 0.17 V [86]	Cyclic voltammetry in H_2/N_2 Low potential in condensing H2/N2 High current / low potential in condensing H2/air Water condensation during shut-down	[78, 90] [83] [60, 78, 89, 90] [91]
Adsorbed nitrogen species	$Pt\cdots NO_x$ ($-NO$,$-NO_2$)	Reduction to ammonium	$Pt\text{-}NO_x + (4+2x)\ H^+ + (3+2x)\ e^- \rightarrow Pt + NH_4^+ + x\ H_2O$	< 0.3 V [96, 97]	Low potential in aqueous solution	[95]
		Oxidation to nitrate	$Pt\text{-}NO_x + (3-x)\ H_2O \rightarrow Pt + NO_3^- + (6-2x)\ H^+ + (5-2x)\ e^-$	> 0.9 V [61]	High potential in aqueous solution Cyclic voltammetry in H_2/N_2 Fuel cell operation in NO_x-free air	[95] [61] [67, 70, 93]
Adsorbed carbon monoxide	Pt···CO	CO oxidation and CO_2 desorption	$Pt\text{-}CO_{ads} + H_2O \rightarrow 2Pt + CO_2 + H^+ + e^-$ $Pt\text{-}CO_{ads} + Pt\text{-}OH_{ads} \rightarrow 2Pt + CO_2 + H^+ + e^-$	> 0.40 V [110] > 0.68 V [47]	External air bleeding Internal air bleed High current / high anode potential pulses	[51, 116, 123-124, 131-132] [102-105, 122, 134-135, 138] [131, 134, 139-141]
Change of ionomer structure	Ionomer adsorption on catalyst	Desorption of sulfonate groups	$Pt\text{-}RSO_3^-{}_{ads} \rightarrow Pt + RSO_3^-$	< 0.2 V [142]	Low potential and high humidity	[142, 145]
	Dense ionomer layer	Relaxation of ionomer structure	Change of ionomer morphology	N/A	Nitrogen purging at high temperature	[143]
Ionomer contamination	NH_4^+, Na^+, Ca^{2+}, Mg^{2+}	Removal of ion contamination	Dissolution in product water	N/A	High current fuel cell operation	[67, 148]
Catalyst support oxidation	More hydrophilic catalyst layer	Reduction of oxygen containing surface groups	$R_2C{=}O + H^+ + e^- \rightarrow R_2C\text{-}OH$ $R_2C\text{-}OH + 2H^+ + 2e^- \rightarrow R_2CH + H2O$	< 0.6 V [167]	Hydrogen pump operation	[47-48]
Water management	Electrode flooding	Water removal	Remove water from pores in catalyst layer and gas diffusion layer	N/A	Shut-down and restart of fuel cell Cathode gas purge	[13, 218, 219] [9, 46, 217, 220-222, 224-225]
	Ionomer dehydration	Rehydration of Ionomer	Increase ionic conductivity	N/A	Fuel cell operation using highly humidified reactant gases High current fuel cell operation	[209, 223] [223]

Originally published on: *Journal of Power Sources 488 (2021) 229375*
DOI: 10.1016/j.jpowsour.2020.229375
https://doi.org/10.1016/j.jpowsour.2020.229375

It is obvious that specific recovery procedures for different reversible performance losses are required to enable high efficiency, reliable characterization and understanding of degradation mechanisms in PEMFCs. Thereby, the following conclusions can be made:

- Highly stable (3D) **platinum oxides** can be reduced combining low cathode potential (0.3 V) and reductive atmosphere using hydrogen permeated from the anode. Hydrogen pump mode using an external power supply can improve and accelerate the recovery.
- **Sulfur poisoning** caused by H_2S, SO_2, and COS requires high electrode potentials of 1.1 V to oxidize Pt-S on the catalyst surface. The resulting sulfate anions have to be desorbed and removed from the catalyst.
- Desorption of **sulfate and sulfonate** anions from sulfur poisoning as well as from membrane degradation takes place at low potentials of about 0.1 V and a subsequent high current fuel cell operation using fully humidified reactants can remove the ions from the catalyst layer. For ultra-low loaded anodes, sulfate anions can also be removed by shut-down and start-up of the cell.
- Catalyst poisoning by **nitrogen oxides** can be slowly recovered by fuel cell operation in neat air. Oxidation of NO_x to nitrate at cathode potentials higher than 0.75 V can accelerate recovery.
- **CO poisoning** can be recovered in high current fuel cell operation by chemical CO oxidation using conditions with increased oxygen permeation (high temperature, pressure, and humidity). The recovery effect is assisted by electrochemical CO oxidation at high anode potentials.
- Slow performance losses addressed to **ionomer structure changes** can be caused by absorption of ionomer sulfonate groups on the catalyst surface at low RH operation. Recovery requires operation at low electrode potentials at high RH or by thermal treatment. Moreover, prolonged high humidity operation can lead to ionomer relaxation leading to tightening of meso-pores leading to mass transport losses as well.
- Trace **contamination by NH_3** is recoverable by neat hydrogen operation at high current density. Prolonged exposures to NH_3 lead to irreversible catalyst layer changes.
- Reversible **catalyst support degradation** and recovery of resulting performance losses are not studied in detail, but several studies mentioned that low potential and reductive atmosphere can reduce surface oxides on carbon supports.
- Recovery of reversible performance losses caused by the **water management** requires water removal and flooding prevention, mainly realized by gas purging, humidity regulation, and cell shut-down with temperature drop.

Consequently, the procedure to recover all reversible performance losses are depending on the application, the operating conditions, the excess to contaminations and the cell, stack or system history. Table 4 summarizes the recommended recovery procedures depending on the available reversible degradation mechanisms during operation. These procedures can be combined to recover losses caused by different procedures.

Table 4: Recommended recovery procedures for reversible degradation mechanisms

Reversible degradation mechanism	Electrode	Laboratory recovery	System recovery
Pt oxidation	**Cathode**	1. Low cathode potential (0.3 V) 2. Hydrogen on cathode	Stop air supply and maintain H_2 supply (Hydrogen permeation to cathode)

Originally published on: *Journal of Power Sources 488 (2021) 229375*
DOI: 10.1016/j.jpowsour.2020.229375
https://doi.org/10.1016/j.jpowsour.2020.229375

		(+hydrogen pump mode)	
Sulfur poisoning by H_2S, SO_2, COS	**Anode + Cathode**	Fast potential cycling in H_2 / N_2 atmosphere between 0.1 and 1.1 V	Fast potential cycling in H_2 / in-situ N_2 atmosphere between 0.1 and 1.1 V
Sulfate and sulfonate adsorption on catalyst	**Anode + Cathode**	1. Low potentials (0.1 V) for desorption 2. High current fuel cell operation using fully humidified reactants or cell shut-down /start-up to remove ions	Stop air supply and maintain H_2 supply (Hydrogen permeation to cathode)
Nitrogen oxide poisoning	**Cathode**	Potential cycling in H_2 / N_2 atmosphere between 0.1 and 1.1 V	Fuel cell operation at high cathode potential (e.g. idling operation)
CO poisoning	**Anode**	High current density fuel cell operation under high temperature, high pressure and high humidity	
Ionomer structure changes at nano-scale	**Cathode/membrane**	High current fuel cell operation using highly humidified gases	
		Thermal treatment	Low potentials during shut-down periods
Ionomer structure changes at meso-scale (porosity)	**Cathode**	Exposure to hot dry N2 (more effective than air)	Exposure to hot dry air
NH_3 contamination	**Cathode**	High current fuel cell operation	
Catalyst support degradation	**Cathode**	Low potential and reductive atmosphere	
Water management	**Anode + Cathode**	Gas purging, cell shut-down with temperature drop	
		Extra devices for water removal (e.g. electroosmotic pump, sequential exhausting device)	-

Glossary:

PEMFC polymer electrolyte membrane fuel cell
ICE internal combustion engine
PGM platinum group metal
CRM critical raw material
FC-DLC Fuel cell dynamic load cycle
FCEV fuel cell electric vehicle
MEA membrane electrode assembly
RHE reversible hydrogen electrode
PFSA perfluorosulfonic acid
ORR oxygen reduction reaction
HOR hydrogen oxidation reaction
CL Catalyst layer
CV cyclic voltammetry
ECSA electrochemical active surface area
SMR steam methane reforming
COS carbonyl sulfide
OCV open circuit voltage

Originally published on: *Journal of Power Sources 488 (2021) 229375*
DOI: 10.1016/j.jpowsour.2020.229375
https://doi.org/10.1016/j.jpowsour.2020.229375

RH Relative humidity
GDL Gas diffusion layer
FTCS Fault tolerant control strategy

8 Acknowledgement

This project has received funding from the Fuel Cells and Hydrogen 2 Joint Undertaking under grant agreement No. 875025 (FURTHER-FC) and No. 779565 (ID-Fast). This Joint Undertaking receives support from the European Union's Horizon 2020 research and innovation programme. Qian Zhang gratefully acknowledges financial support from China Scholarship Council.

9 References

[1] I. Staffell, D. Scamman, A. Velazquez Abad, P. Balcombe, P.E. Dodds, P. Ekins, N. Shah, K.R. Ward, Energy & Environmental Science, 12 (2019) 463-491.
[2] D. Hart, F. Lehner, S. Jones, J. Lewis, M. Klippenstein, in, E4tech, 2018.
[3] U. DOE, in, Technical report: US Department of Energy, 2016.
[4] S.T. Thompson, D. Papageorgopoulos, Nature Catalysis, 2 (2019) 558-561.
[5] A. Kongkanand, M.F. Mathias, J Phys Chem Lett, 7 (2016) 1127-1137.
[6] https://ec.europa.eu/growth/sectors/raw-materials/specific-interest/critical_en
[7] G.P. Keeley, S. Cherevko, K.J. Mayrhofer, ChemElectroChem, 3 (2016) 51-54.
[8] A. Kongkanand, N.P. Subramanian, Y. Yu, Z. Liu, H. Igarashi, D.A. Muller, ACS Catalysis, 6 (2016) 1578-1583.
[9] P. Gazdzicki, J. Mitzel, A.M. Dreizler, M. Schulze, K.A. Friedrich, Fuel Cells, 18 (2018) 270-278.
[10] R. Borup, J. Meyers, B. Pivovar, Y.S. Kim, R. Mukundan, N. Garland, D. Myers, M. Wilson, F. Garzon, D. Wood, P. Zelenay, K. More, K. Stroh, T. Zawodzinski, J. Boncella, J.E. McGrath, M. Inaba, K. Miyatake, M. Hori, K. Ota, Z. Ogumi, S. Miyata, A. Nishikata, Z. Siroma, Y. Uchimoto, K. Yasuda, K.-i. Kimijima, N. Iwashita, Chemical Reviews, 107 (2007) 3904-3951.
[11] S. Zhang, X.-Z. Yuan, J.N.C. Hin, H. Wang, K.A. Friedrich, M. Schulze, Journal of Power Sources, 194 (2009) 588-600.
[12] S. Cleghorn, D. Mayfield, D. Moore, J. Moore, G. Rusch, T. Sherman, N. Sisofo, U. Beuscher, Journal of Power Sources, 158 (2006) 446-454.
[13] P. Gazdzicki, J. Mitzel, D. Garcia Sanchez, M. Schulze, K.A. Friedrich, Journal of Power Sources, 327 (2016) 86-95.
[14] G. Tsotridis, A. Pilenga, G. De Marco, T. Malkow, JRC Science for Policy Report, JRC99115 (2015).
[15] L. Topal, C. Harms, A. Kabza, J. Hunger, in: A test module of the European Stack-Test project (FCH-JU grant no. 303445), 2015.
[16] S. Kundu, M. Fowler, L.C. Simon, R. Abouatallah, Journal of Power Sources, 182 (2008) 254-258.
[17] P. Piela, J. Mitzel, Journal of Power Sources, 292 (2015) 95-103.
[18] J. Mitzel, E. Gülzow, A. Kabza, J. Hunger, S.S. Araya, P. Piela, I. Alecha, G. Tsotridis, International Journal of Hydrogen Energy, 41 (2016) 21415-21426.
[19] M.A. Rubio, A. Urquia, S. Dormido, International Journal of Hydrogen Energy, 35 (2010) 2586-2590.
[20] F.A. de Bruijn, V.A.T. Dam, G.J.M. Janssen, Fuel Cells, 8 (2008) 3-22.
[21] B.D. Gould, G. Bender, K. Bethune, S. Dorn, O.A. Baturina, R. Rocheleau, K.E. Swider-Lyons, Journal of The Electrochemical Society, 157 (2010) B1569-B1577.
[22] S.G. Rinaldo, W. Lee, J. Stumper, M. Eikerling, Electrocatalysis, 5 (2014) 262-272.
[23] S. Yang, S. Choi, Y. Kim, J. Yoon, S. Im, H.S. Choo, International Journal of Automotive Technology, 20 (2019) 1113-1121.

[24] B.R. Shrestha, A.P. Yadav, A. Nishikata, T. Tsuru, Electrochimica Acta, 56 (2011) 9714-9720.
[25] R.K. Ahluwalia, S. Arisetty, X. Wang, X. Wang, R. Subbaraman, S.C. Ball, S. DeCrane, D.J. Myers, Journal of The Electrochemical Society, 160 (2013) F447-F455.
[26] R.M. Darling, J.P. Meyers, Journal of The Electrochemical Society, 150 (2003) A1523-A1527.
[27] H. Xu, R. Kunz, J.M. Fenton, Electrochemical and Solid-State Letters, 10 (2007) B1-B5.
[28] G. Jerkiewicz, G. Vatankhah, J. Lessard, M.P. Soriaga, Y.-S. Park, Electrochimica Acta, 49 (2004) 1451-1459.
[29] E.L. Redmond, B.P. Setzler, F.M. Alamgir, T.F. Fuller, Phys Chem Chem Phys, 16 (2014) 5301-5311.
[30] T. Nagai, H. Murata, Y. Morimoto, ECS Transactions, 33 (2010) 125-130.
[31] D.E. Ramaker, A. Korovina, V. Croze, J. Melke, C. Roth, Phys Chem Chem Phys, 16 (2014) 13645-13653.
[32] M. Teliska, W.E. O'Grady, D.E. Ramaker, Journal of Physical Chemistry, 109 (2005) 8076-8084.
[33] D.A. Harrington, Journal of Electroanalytical Chemistry, 420 (1997) 101-109.
[34] S. Shibata, M.P. Sumino, Electrochimica Acta, 20 (1975) 739-746.
[35] Y. Liu, M. Mathias, J. Zhang, Electrochemical and Solid-State Letters, 13 (2010) B1-B3.
[36] C.H. Paik, T.D. Jarvi, W.E. O'Grady, Electrochemical and Solid-State Letters, 7 (2004) A82-A84.
[37] M. Zago, A. Baricci, A. Bisello, T. Jahnke, H. Yu, R. Maric, P. Zelenay, A. Casalegno, Journal of Power Sources, 455 (2020).
[38] B.E. Conway, B. Barnett, H. Angerstein-Kozlowska, B.V. Tilak, The Journal of Chemical Physics, 93 (1990) 8361-8373.
[39] F.A. Uribe, T.A. Zawodzinski, Electrochimica Acta, 47 (2002) 3799-3806.
[40] A.A. Topalov, S. Cherevko, A.R. Zeradjanin, J.C. Meier, I. Katsounaros, K.J.J. Mayrhofer, Chem. Sci., 5 (2014) 631-638.
[41] H.S. Casalongue, S. Kaya, V. Viswanathan, D.J. Miller, D. Friebel, H.A. Hansen, J.K. Nørskov, A. Nilsson, H. Ogasawara, Nature Communications, 4 (2013).
[42] Y. Zhang, S. Chen, Y. Wang, W. Ding, R. Wu, L. Li, X. Qi, Z. Wei, Journal of Power Sources, 273 (2015) 62-69.
[43] X. Zhang, L. Guo, H. Liu, Journal of Power Sources, 296 (2015) 327-334.
[44] J.P. Owejan, J.E. Owejan, W. Gu, Journal of The Electrochemical Society, 160 (2013) F824-F833.
[45] S.R. Dhanushkodi, M. Tam, S. Kundu, M.W. Fowler, M.D. Pritzker, Journal of Power Sources, 240 (2013) 114-121.
[46] S.R. Dhanushkodi, S. Kundu, M.W. Fowler, M.D. Pritzker, Journal of Power Sources, 245 (2014) 1035-1045.
[47] H.S. Choo, D.K. Chun, J.H. Lee, H.S. Shin, S.K. Lee, Y.S. Park, B.K. Ahn, in: SAE Technical Paper Series, 2015.
[48] H.S. Choo, D.K. Chun, H.S. Shin, S.K. Lee, J.H. Lee, in: H.M. Company (Ed.), US, 2018, pp. 17.
[49] U. Izquierdo, V.L. Barrio, J.F. Cambra, J. Requies, M.B. Güemez, P.L. Arias, G. Kolb, R. Zapf, A.M. Gutiérrez, J.R. Arraibi, International Journal of Hydrogen Energy, 37 (2012) 7026-7033.
[50] D.B. Levin, R. Chahine, International Journal of Hydrogen Energy, 35 (2010) 4962-4969.
[51] X. Cheng, Z. Shi, N. Glass, L. Zhang, J. Zhang, D. Song, Z.-S. Liu, H. Wang, J. Shen, Journal of Power Sources, 165 (2007) 739-756.
[52] A. Collier, H. Wang, X. Ziyuan, J. Zhang, D. Wilkinson, International Journal of Hydrogen Energy, 31 (2006) 1838-1854.
[53] J. Zhang, H. Wang, D.P. Wilkinson, D. Song, J. Shen, Z.-S. Liu, Journal of Power Sources, 147 (2005) 58-71.
[54] J.M. Moore, P.L. Adcock, J.B. Lakeman, G.O. Mepsted, Journal of Power Sources, 85 (2000) 254-260.
[55] M. Opu, M. Ohashi, H.S. Cho, C.S. Macomber, H.N. Dinh, J.W. Van Zee, ECS Transactions, 50 (2012) 619-634.

[56] H. Wang, C. Macomber, J. Christ, G. Bender, B. Pivovar, H.N. Dinh, Electrocatalysis, 5 (2013) 62-67.
[57] T.V. Reshetenko, J. St-Pierre, Journal of Power Sources, 333 (2016) 237-246.
[58] K. Bethune, J. St-Pierre, J.M. LaManna, D.S. Hussey, D.L. Jacobson, The Journal of Physical Chemistry C, 124 (2020) 24052-24065.
[59] J. Fu, M. Hou, C. Du, Z. Shao, B. Yi, Journal of Power Sources, 187 (2009) 32-38.
[60] Y. Nagahara, S. Sugawara, K. Shinohara, Journal of Power Sources, 182 (2008) 422-428.
[61] F. Jing, M. Hou, W. Shi, J. Fu, H. Yu, P. Ming, B. Yi, Journal of Power Sources, 166 (2007) 172-176.
[62] W. Shi, B. Yi, M. Hou, F. Jing, H. Yu, P. Ming, Journal of Power Sources, 164 (2007) 272-277.
[63] B.D. Gould, O.A. Baturina, K.E. Swider-Lyons, Journal of Power Sources, 188 (2009) 89-95.
[64] M.-V. Mathieu, M. Primet, Applied Catalysis, 9 (1984) 361-370.
[65] E. Najdeker, E. Bishop, Electroanalytical Chemistry and Interfacial Electrochemistry, 41 (1973) 79-87.
[66] R. Mohtadi, W.K. Lee, J.W. Van Zee, Applied Catalysis B: Environmental, 56 (2005) 37-42.
[67] F.H. Garzon, T. Lopes, T. Rockward, J.-M. Sansiñena, B. Kienitz, R. Mukundan, T. Springer, ECS Transactions, 25 (2009) 1575-1583.
[68] A.Q. Contractor, H. Lal, Journal of Electroanalytical Chemistry, 93 (1978) 99-107.
[69] E.S. Argano, S.S. Randhava, A. Rehmat, Transactions of the Faraday Society, 65 (1968) 552-560.
[70] R. Mohtadi, W.k. Lee, J.W. Van Zee, Journal of Power Sources, 138 (2004) 216-225.
[71] R. Mohtadi, W.k. Lee, S. Cowan, J.W. Van Zee, M. Murthy, Electrochemical and Solid-State Letters, 6 (2003) A272-A274.
[72] A.Q. Contractor, H. Lal, Journal of Electroanalytical Chemistry, 96 (1979) 175-181.
[73] I.G. Urdampilleta, F.A. Uribe, T. Rockward, E.L. Brosha, B.S. Pivovar, F.H. Garzon, ECS Transactions, 11 (2007) 831-842.
[74] W. Shi, B. Yi, M. Hou, F. Jing, P. Ming, Journal of Power Sources, 165 (2007) 814-818.
[75] T. Loucka, Electroanalytical Chemistry and Interfacial Electrochemistry, 31 (1971) 319-332.
[76] Y. Wang, H. Yan, E.f. Wang, Journal of Electroanalytical Chemistry, 497 (2001) 163-167.
[77] M. Inaba, T. Kinumoto, M. Kiriake, R. Umebayashi, A. Tasaka, Z. Ogumi, Electrochimica Acta, 51 (2006) 5746-5753.
[78] A. Kabasawa, H. Uchida, M. Watanabe, Electrochemical and Solid-State Letters, 11 (2008) B190-B192.
[79] J. Healy, C. Hayden, T. Xie, K. Olson, R. Waldo, M. Brundage, H. Gasteiger, J. Abbott, Fuel Cells, 5 (2005) 302-308.
[80] K. Teranishi, K. Kawata, S. Tsushima, S. Hirai, Electrochemical and Solid-State Letters, 9 (2006) A475-A477.
[81] N.E. Cipollini, ECS Transactions, 11 (2007) 1071-1082.
[82] F.D. Coms, ECS Transactions, 16 (2008) 235-255.
[83] S. Sugawara, T. Maruyama, Y. Nagahara, S.S. Kocha, K. Shinohra, K. Tsujita, S. Mitsushima, K.-i. Ota, Journal of Power Sources, 187 (2009) 324-331.
[84] J. Zhang, B.A. Litteer, F.D. Coms, R. Makharia, Journal of The Electrochemical Society, 159 (2012) F287-F293.
[85] J. Zhang, B. Litteer, F. Coms, R. Makharia, ECS Transactions, 41 (2011) 1471-1485.
[86] O.A. Baturina, K.E. Swider-Lyons, Journal of The Electrochemical Society, 156 (2009) B1423-B1430.
[87] R. Borup, R. Mukundan, D. Spernjak, D. Langlois, N. Macauley, Y.S. Kim, in: 230th ECS Meeting, Honolulu, Hawaii, United States, 2016.
[88] U.A. Paulus, T.J. Schmidt, H.A. FGasteiger, R.J. Behm, Journal of Electroanalytical Chemistry, 495 (2001) 134-145.
[89] M. Inaba, H. Yamada, R. Umebayashi, M. Sugishita, A. Tasaka, Electrochemistry Communications, 75 (2007) 207-212.

[90] A. Kabasawa, J. Saito, K. Miyatake, H. Uchida, M. Watanabe, Electrochimica Acta, 54 (2009) 2754-2760.
[91] S. Prass, K.A. Friedrich, N. Zamel, Molecules, 24 (2019).
[92] I.P. Kandylas, O.A. Haralampous, G.C. Koltsakis, Industrial & Engineering Chemistry Research, 41 (2002) 5372-5384.
[93] M.C. Bétournay, G. Bonnell, E. Edwardson, D. Paktunc, A. Kaufman, A.T. Lomma, Journal of Power Sources, 134 (2004) 80-87.
[94] D. Yang, J. Ma, L. Xu, M. Wu, H. Wang, Electrochimica Acta, 51 (2006) 4039-4044.
[95] M. Chen, C. Du, J. Zhang, P. Wang, T. Zhu, Journal of Power Sources, 196 (2011) 620-626.
[96] A.C.A. de Vooys, G.L. Beltramo, B. van Riet, J.A.R. van Veen, M.T.M. Koper, Electrochimica Acta, 49 (2004) 1307-1314.
[97] A.J. Bard, Encyclopedia of Electrochemistry of the Elements, Marcel Dekker Inc. NY, 1986.
[98] C.-Y. Lin, W.-T. Hung, C.-T. Wu, K.-C. Ho, Sensors and Actuators B: Chemical, 136 (2009) 32-38.
[99] F.A. Uribe, S. Gottesfeld, T.A. Zawodzinski, Journal of The Electrochemical Society, 149 (2002) A293-A296.
[100] H.J. Soto, W.-k. Lee, J.W. Van Zee, M. Murthy, Electrochemical and Solid-State Letters, 6 (2003) A133-A135.
[101] M. Murthy, M. Esayian, W.-k. Lee, J.W. Van Zee, Journal of The Electrochemical Society, 150 (2003) A29-A34.
[102] G. Bender, M. Angelo, K. Bethune, R. Rocheleau, Journal of Power Sources, 228 (2013) 159-169.
[103] Z. Qi, C. He, A. Kaufman, Electrochemical and Solid-State Letters, 4 (2001) A204-A205.
[104] Z. Qi, C. He, A. Kaufman, Journal of Power Sources, 111 (2002) 239-247.
[105] W. Wang, Journal of Power Sources, 191 (2009) 400-406.
[106] J.M. Rheaume, B. Müller, M. Schulze, Journal of Power Sources, 76 (1998) 60-68.
[107] M. Ciureanu, H. Wang, Journal of The Electrochemical Society, 146 (1999) 4031-4040.
[108] M. Watanabe, S. Motoo, Journal of Electroanalytical Chemistry, 206 (1986) 197-208.
[109] H. Igarashi, T. Fujino, M. Watanabe, Journal of Electroanalytical Chemistry, 391 (1995) 119-123.
[110] G.A. Camara, E.A. Ticianelli, S. Mukerjee, S.J. Lee, J. McBreen, Journal of The Electrochemical Society, 149 (2002) A748-A753.
[111] F.A. de Bruijn, D.C. Papageorgopoulos, E.F. Sitters, G.J.M. Janssen, Journal of Power Sources, 110 (2002) 117-124.
[112] G.J.M. Janssen, Journal of Power Sources, 136 (2004) 45-54.
[113] T.R. Ralph, M.P. Hogarth, Platinum Metals Rev., 46 (2002) 117-135.
[114] T. Gu, W.K. Lee, J.W.V. Zee, Applied Catalysis B: Environmental, 56 (2005) 43-50.
[115] S. Ma, E. Skou, Solid State Ionics, 178 (2007) 615-619.
[116] L.C. Pérez, T. Rajala, J. Ihonen, P. Koski, J.M. Sousa, A. Mendes, International Journal of Hydrogen Energy, 38 (2013) 16286-16299.
[117] Y. Hashimasaa, Y. Matsudaa, M. Akai, ECS Transactions, 26 (2010) 131-142.
[118] H. Matsuyama, K. Matsui, Y. Kitamura, T. Maki, M. Teramoto, Separation and Purification Technology, 17 (1999) 235-241.
[119] T. Iwasita, X. Xia, Journal of Electroanalytical Chemistry, 411 (1996) 95-102.
[120] T. Ioroi, K. Yasuda, Y. Miyazaki, Physical Chemistry Chemical Physics, 4 (2002) 2337-2340.
[121] A.B. Anderson, N.M. Neshev, Journal of The Electrochemical Society, 149 (2002) E383-E388.
[122] J. Zhang, T. Thampan, R. Datta, Journal of The Electrochemical Society, 149 (2002) A765-A772.
[123] S. Gottesfeld, J. Pafford, Journal of The Electrochemical Society, 135 (1988) 2651-2652.
[124] L.-Y. Sung, B.-J. Hwang, K.-L. Hsueh, W.-N. Su, C.-C. Yang, Journal of Power Sources, 242 (2013) 264-272.
[125] M. Murthy, M. Esayian, A. Hobson, S. MacKenzie, W.-k. Lee, J.W. Van Zee, Journal of The Electrochemical Society, 148 (2001) A1141-A1147.
[126] N. Zamel, X. Li, Progress in Energy and Combustion Science, 37 (2011) 292-329.

[127] M. Inaba, M. Sugishita, J. Wada, K. Matsuzawa, H. Yamada, A. Tasaka, Journal of Power Sources, 178 (2008) 699-705.
[128] Z. Jusys, R.J. Behm, J. Phys. Chem. B, 108 (2004) 7893-7901.
[129] V. Stamenkovic, B.N. Grgur, R. P.N., N.M. Markovic, Journal of The Electrochemical Society, 152 (2005) A277-282.
[130] Y. Shao, G. Yin, Y. Gao, Journal of Power Sources, 171 (2007) 558-566.
[131] W.A. Adams, J. Blair, K.R. Bullock, C.L. Gardner, Journal of Power Sources, 145 (2005) 55-61.
[132] T. Tingelöf, L. Hedström, N. Holmström, P. Alvfors, G. Lindbergh, International Journal of Hydrogen Energy, 33 (2008) 2064-2072.
[133] J. Zhang, R. Datta, Electrochemical and Solid-State Letters, 6 (2003) A5-A8.
[134] S. Jiménez, J. Soler, R.X. Valenzuela, L. Daza, Journal of Power Sources, 151 (2005) 69-73.
[135] T.V. Reshetenko, K. Bethune, M.A. Rubio, R. Rocheleau, Journal of Power Sources, 269 (2014) 344-362.
[136] K. Broka, P. Ekdunge, Journal of Applied Electrochemistry, 27 (1997) 117-.
[137] F. Arena, J. Mitzel, R. Hempelmann, Fuel Cells, 13 (2013) 58-64.
[138] K.K. Bhatia, C.-Y. Wang, Electrochimica Acta, 49 (2004) 2333-2341.
[139] J. Zhang, R. Datta, Journal of The Electrochemical Society, 149 (2002) A1423-A1431.
[140] A.H. Thomason, T.R. Lalk, A.J. Appleby, Journal of Power Sources, 135 (2004) 204-211.
[141] L.P.L. Carrette, K.A. Friedrich, M. Huber, U. Stimming, Physical Chemistry Chemical Physics, 3 (2001) 320-324.
[142] S. Jomori, K. Komatsubara, N. Nonoyama, M. Kato, T. Yoshida, Journal of The Electrochemical Society, 160 (2013) F1067-F1073.
[143] D.A. Langlois, A.S. Lee, N. Macauley, S. Maurya, M.E. Hawley, S.D. Yim, Y.S. Kim, Journal of Power Sources, 396 (2018) 345-354.
[144] S. Kreitmeier, M. Michiardi, A. Wokaun, F.N. Büchi, Electrochimica Acta, 80 (2012) 240-247.
[145] A. Kongkanand, V. Yarlagadda, T. Garrick, T.E. Moylan, W. Gu, ECS Transactions, 75 (2016) 25-34.
[146] J. Shan, P. Gazdzicki, R. Lin, M. Schulze, K.A. Friedrich, Energy, 128 (2017) 357-365.
[147] Y.-H. Lai, C.K. Mittelsteadt, C.S. Gittleman, D.A. Dillard, Journal of Fuel Cell Science and Technology, 6 (2009) 021002-021001 - 021002-021013.
[148] Y.A. Gomez, A. Oyarce, G. Lindbergh, C. Lagergren, Journal of The Electrochemical Society, 165 (2018) F189-F197.
[149] K. Hongsirikarn, J.G. Goodwin, S. Greenway, S. Creager, Journal of Power Sources, 195 (2010) 7213-7220.
[150] R. Halseid, P.J.S. Vie, R. Tunold, Journal of Power Sources, 154 (2006) 343-350.
[151] J. Zhu, J. Tan, Q. Pan, Z. Liu, Q. Hou, Energy, 189 (2019).
[152] S. Sharma, B.G. Pollet, Journal of Power Sources, 208 (2012) 96-119.
[153] H.-S. Choo, T. Kinumoto, M. Nose, K. Miyazaki, T. Abe, Z. Ogumi, Journal of Power Sources, 185 (2008) 740-746.
[154] M. Khorshidian, M. Sedighi, Iranian Journal of Hydrogen & Fuel Cell, 6 (2019) 91-115.
[155] J. Liu, Z. Hou, Carbon Corrosion in Polymer Electrolyte Membrane Fuel Cell Catalysts and its Mitigation Strategies, in: Eco-and Renewable Energy Materials, Springer, 2013, pp. 53-72.
[156] T. Zhang, P. Wang, H. Chen, P. Pei, Applied energy, 223 (2018) 249-262.
[157] H.S. Choo, T. Kinumoto, S.-K. Jeong, Y. Iriyama, T. Abe, Z. Ogumi, Journal of The Electrochemical Society, 154 (2007) B1017-B1023.
[158] N. Linse, G.G. Scherer, A. Wokaun, L. Gubler, Journal of Power Sources, 219 (2012) 240-248.
[159] M.R. Tarasevich, V.A. Bogdanovskaya, N.M. Zagudaeva, Journal of Electroanalytical Chemistry and Interfacial Electrochemistry, 223 (1987) 161-169.
[160] K. Kinoshita, J. Bett, Carbon, 11 (1973) 403-411.
[161] N. Giordano, E. Passalacqua, L. Pino, A. Arico, V. Antonucci, M. Vivaldi, K. Kinoshita, Electrochimica Acta, 36 (1991) 1979-1984.

[162] G. Álvarez, F. Alcaide, O. Miguel, P.L. Cabot, M.V. Martínez-Huerta, J.L.G. Fierro, Electrochimica Acta, 56 (2011) 9370-9377.
[163] A.P. Young, V. Colbow, D. Harvey, E. Rogers, S. Wessel, Journal of The Electrochemical Society, 160 (2013) F381-F388.
[164] J. Kim, J. Lee, Y. Tak, Journal of Power Sources, 192 (2009) 674-678.
[165] Z. Zhao, L. Castanheira, L. Dubau, G. Berthomé, A. Crisci, F. Maillard, Journal of Power Sources, 230 (2013) 236-243.
[166] M.L. Perry, T. Patterson, C. Reiser, Ecs Transactions, 3 (2006) 783.
[167] Y. Shao, J. Wang, R. Kou, M. Engelhard, J. Liu, Y. Wang, Y. Lin, 54 (2009) 3109-3114.
[168] M. Nose, T. Kinumoto, H.-S. Choo, K. Miyazaki, T. Abe, Z. Ogumi, Chemistry Letters, 38 (2009) 788-789.
[169] Z.R. Yue, W. Jiang, L. Wang, S.D. Gardner, C.U. Pittman, Carbon, 37 (1999) 1785-1796.
[170] K.H. Kangasniemi, D.A. Condit, T.D. Jarvi, Journal of The Electrochemical Society, 151 (2004).
[171] D. Rivin, Rubber Chemistry and Technology, 36 (1963) 729-739.
[172] N.L. Weinberg, T.B. Reddy, 3 (1973) 73-75.
[173] K. Horie, M. Hiromichi, I. Mita, Fibre Science and Technology, 9 (1976) 253-264.
[174] L. Castanheira, W.O. Silva, F.H.B. Lima, A. Crisci, L. Dubau, F. Maillard, ACS Catalysis, 5 (2015) 2184-2194.
[175] N. Laine, F. Vastola, P. Walker Jr, The Journal of physical chemistry, 67 (1963) 2030-2034.
[176] M.T. Coltharp, N. Hackerman, The Journal of Physical Chemistry, 72 (1968) 1171-1177.
[177] L. Castanheira, L. Dubau, M. Mermoux, G. Berthomé, N. Caqué, E. Rossinot, M. Chatenet, F. Maillard, ACS Catalysis, 4 (2014) 2258-2267.
[178] J.D. Fairweather, D. Spernjak, A.Z. Weber, D. Harvey, S. Wessel, D.S. Hussey, D.L. Jacobson, K. Artyushkova, R. Mukundan, R.L. Borup, 160 (2013) F980-F993.
[179] L.C. Colmenares, A. Wurth, Z. Jusys, R.J. Behm, 190 (2009) 14-24.
[180] F.-Y. Zhang, D. Spernjak, A.K. Prasad, S.G. Advani, Journal of The Electrochemical Society, 154 (2007).
[181] F. Maillard, A. Bonnefont, F. Micoud, 13 (2011) 1109-1111.
[182] L. Dubau, M. Lopez-Haro, L. Castanheira, J. Durst, M. Chatenet, P. Bayle-Guillemaud, L. Guétaz, N. Caqué, E. Rossinot, F. Maillard, Applied Catalysis B: Environmental, 142-143 (2013) 801-808.
[183] X. Yu, S. Ye, Journal of Power Sources, 172 (2007) 145-154.
[184] Y. Shao, G. Yin, J. Zhang, Y. Gao, Electrochimica Acta, 51 (2006) 5853-5857.
[185] M.J. Bleda-Martínez, D. Lozano-Castelló, E. Morallon, D. Cazorla-Amorós, A. Linares-Solano, Carbon, 44 (2006) 2642-2651.
[186] K.A. Kun, 3 (1965) 1833-1843.
[187] A.B. Fuertes, T.A. Centeno, Journal of Materials Chemistry, 15 (2005) 1079-1083.
[188] X. Wang, J.S. Lee, Q. Zhu, J. Liu, Y. Wang, S. Dai, Chemistry of Materials, 22 (2010) 2178-2180.
[189] F. Hasché, M. Oezaslan, P. Strasser, Physical Chemistry Chemical Physics, 12 (2010) 15251-15258.
[190] L. Li, Y. Xing, Journal of Power Sources, 178 (2008) 75-79.
[191] L.L. Van Dine, M.M. Steinbugler, C.A. Reiser, G.W. Scheffler, in, Google Patents, 2003.
[192] D. Yang, M. Steinbugler, R. Sawyer, L. Van Dine, C. Reiser, in, Google Patents, 2003.
[193] A. Amirfazli, S. Asghari, M. Sarraf, Energy, 145 (2018) 141-151.
[194] S.Y. Kim, W.N. Kim, Journal of power Sources, 166 (2007) 430-434.
[195] A.Z. Weber, J. Newman, Chemical Reviews, 104 (2004) 4679-4726.
[196] J.P. Owejan, J.J. Gagliardo, J.M. Sergi, S.G. Kandlikar, T.A. Trabold, International Journal of Hydrogen Energy, 34 (2009) 3436-3444.
[197] S. Litster, C.R. Buie, T. Fabian, J.K. Eaton, J.G. Santiago, Journal of The Electrochemical Society, 154 (2007) B1049-B1058.
[198] S. Tsushima, S. Hirai, Progress in Energy and Combustion Science, 37 (2011) 204-220.
[199] C.-Y. Wang, Chemical Reviews, 104 (2004) 4727-4766.

[200] D.G. Sanchez, T. Ruiu, K.A. Friedrich, J. Sanchez-Monreal, M. Vera, Journal of The Electrochemical Society, 163 (2016) F150-F159.
[201] P. García-Salaberri, D. Sánchez, P. Boillat, M. Vera, K.A. Friedrich, Journal of power sources, 359 (2017) 634-655.
[202] J.H. Nam, K.-J. Lee, G.-S. Hwang, C.-J. Kim, M. Kaviany, International Journal of Heat and Mass Transfer, 52 (2009) 2779-2791.
[203] N. Yousfi-Steiner, P. Moçotéguy, D. Candusso, D. Hissel, A. Hernandez, A. Aslanides, Journal of Power Sources, 183 (2008) 260-274.
[204] M. Ji, Z. Wei, Energies, 2 (2009) 1057-1106.
[205] M.A. Hickner, C.H. Fujimoto, C.J. Cornelius, 47 (2006) 4238-4244.
[206] H. Takata, N. Mizuno, M. Nishikawa, S. Fukada, M. Yoshitake, International Journal of Hydrogen Energy, 32 (2007) 371-379.
[207] O. Ijaodola, Z. El-Hassan, E. Ogungbemi, F. Khatib, T. Wilberforce, J. Thompson, A. Olabi, Energy, 179 (2019) 246-267.
[208] X. Ye, M. Douglas Levan, Journal of Membrane Science, 221 (2003) 147-161.
[209] J. Stumper, M. Löhr, S. Hamada, Journal of Power Sources, 143 (2005) 150-157.
[210] Y. Sone, P. Ekdunge, D. Simonsson, Journal of the Electrochemical Society, 143 (1996) 1254-1259.
[211] H. Görgün, M. Arcak, F. Barbir, Journal of Power Sources, 157 (2006) 389-394.
[212] J.-M. Le Canut, R.M. Abouatallah, D.A. Harrington, Journal of The Electrochemical Society, 153 (2006) A857-A864.
[213] D. Natarajan, T. Van Nguyen, AIChE Journal, 51 (2005) 2587-2598.
[214] M. Tomas, I.S. Biswas, P. Gazdzicki, L. Kullova, M. Schulze, Materials for Renewable and Sustainable Energy, 6 (2017) 20.
[215] P. Rodatz, F. Büchi, C. Onder, L. Guzzella, Journal of Power Sources, 128 (2004) 208-217.
[216] R. Eckl, W. Zehtner, C. Leu, U. Wagner, Journal of Power Sources, 138 (2004) 137-144.
[217] J.P. Owejan, T.A. Trabold, J.J. Gagliardo, D.L. Jacobson, R.N. Carter, D.S. Hussey, M. Arif, 171 (2007) 626-633.
[218] Z. Qi, H. Tang, Q. Guo, B. Du, 161 (2006) 864-871.
[219] L. Guétaz, S. Escribano, O. Sicardy, Journal of Power Sources, 212 (2012) 169-178.
[220] E.E. Kimball, J.B. Benziger, Y.G. Kevrekidis, 10 (2010) 530-544.
[221] S. Zhang, X.-Z. Yuan, J.N.C. Hin, H. Wang, J. Wu, K.A. Friedrich, M. Schulze, Journal of Power Sources, 195 (2010) 1142-1148.
[222] S. Zhai, S. Zhou, P. Sun, F. Chen, J. Niu, Journal of Fuel Cell Science and Technology, 9 (2012).
[223] J. Cho, H.-S. Kim, K. Min, 185 (2008) 118-128.
[224] C. Lebreton, M. Benne, C. Damour, N. Yousfi-Steiner, B. Grondin-Perez, D. Hissel, J.-P. Chabriat, 40 (2015) 10636-10646.
[225] W. Schmittinger, A. Vahidi, Journal of Power Sources, 180 (2008) 1-14.
[226] T. Van Nguyen, M.W. Knobbe, Journal of Power Sources, 114 (2003) 70-79.
[227] D.G. Strickland, S. Litster, J.G. Santiago, 174 (2007) 272-281.
[228] X. Zhang, Y. Yang, L. Guo, H. Liu, International Journal of Hydrogen Energy, 42 (2017) 4699-4705.
[229] M.M. Mench, C.Y. Wang, M. Ishikawa, Journal of The Electrochemical Society, 150 (2003).
[230] I. Pivac, F. Barbir, Fuel Cells, 20 (2020) 185-195.
[231] M. Schulze, N. Wagner, T. Kaz, K.A. Friedrich, Electrochimica Acta, 52 (2007) 2328-2336.